INPP4B overexpression and c-KIT downregulation in human achalasia

Journal:	*Neurogastroenterology and Motility*
Manuscript ID	NMO-00426-2017.R1
Manuscript Type:	Original Article
Date Submitted by the Author:	n/a
Complete List of Authors:	Bonora, Elena; Medical Genetics Unit, St.Orsola Malpighi Bianco, Francesca; University of Bologna Stanzani, Agnese; University of Bologna, Medical and Surgical Sciences Giancola, Fiorella; University of Bologna, Department of Veterinary Medical SCiences Astolfi, Annalisa; University of Bologna, Medical and Surgical Sciences Indio, Valentina; University of Bologna, Medical and Surgical Sciences Evangelisti, Cecilia Martelli, Alberto; University of Bologna, DIBINEM Boschetti, Elisa; University of Bologna, Medical and Surgical Sciences Lugaresi, Marialuisa; University of Bologna, Medical and Surgical Sciences Ioannou, Alexandros; University of Bologna, Medical and Surgical Sciences Torresan, Francesco Stanghellini, Vincenzo Clavenzani, Paolo Seri, Marco; Medical Genetics Unit, St.Orsola Malpighi Moonen, An van Beek, Kim; KU Leuven Wouters, Mira M.; Katholieke Universiteit Leuven Faculteit Wetenschappen, Translational Research in Gastrointestin Boeckxstaens, Guy; KUL, Zaninotto, Giovanni Mattioli, Sandro; University of Bologna, Medical and Surgical Sciences De Giorgio, Roberto; University of Bologna, Medical and Surgical Sciences
Key Words:	Achalasia, c-Kit, INPP4B, transcriptome, cell signaling

INPP4B overexpression and *c-KIT* downregulation in human achalasia

Running title: *INPP4B and c-KIT dysregulation in achalasia*

Elena Bonora[1], Francesca Bianco[1,2], Agnese Stanzani[1,2], Fiorella Giancola[1,2,3], Annalisa Astolfi[4], Valentina Indio[4], Cecilia Evangelisti[5], Alberto Maria Martelli[5], Elisa Boschetti[1,3], Marialuisa Lugaresi[1], Alexandros Ioannou[1], Francesco Torresan[6], Vincenzo Stanghellini[1], Paolo Clavenzani[2], Marco Seri[1], An Moonen[7], Kim Van Beek[7], Mira Wouters[7], Guy E. Boeckxstaens[7], Giovanni Zaninotto[8], Sandro Mattioli[1] and Roberto De Giorgio[9]

[1] Department of Medical and Surgical Sciences, DIMEC, University of Bologna and St. Orsola-Malpighi Hospital, Bologna, Italy.

[2] Department of Medical and Veterinary Sciences, DIMEVET, University of Bologna, Bologna, Italy.

[3] Centro di Ricerca Biomedica Applicata, St.Orsola-Malpighi Hospital, Bologna, Italy

[4] Interdepartmental Center for Cancer Research "G. Prodi" (CIRC), University of Bologna, Bologna, Italy.

[5] Department of Experimental Medicine, DIMES, University of Bologna, Bologna, Italy.

[6] Department of Digestive System, St. Orsola-Malpighi Hospital, Bologna, Italy.

[7] Translational Research in GastroIntestinal Disorders (TARGID), Department of Clinical and Experimental Medicine, KU Leuven University, Belgium.

[8] Division of Surgery, Imperial College London, London, United Kingdom.

[9] Department of Medical Sciences, Nuovo Arcispedale S.Anna at Cona (Ferrara), University of Ferrara, Italy.

Funding

FB is recipient of a Telethon fellowship. This work was supported by grant GGP15171 from Fondazione Telethon and University of Bologna (RFO funds) to EB and RDeG. RDeG received research grants from Fondazione Del Monte of Bologna and Ravenna. The funding bodies did not influence the content of this article.

Abbreviations

CPM - count per million, GO - gene ontology, LES - lower esophageal sphincter, MEV - multiple experiment viewer, ICC - interstitial cells of Cajal, INPP4B - inositol polyphosphate-4-phosphatase, type II B.

Correspondence address:

Roberto De Giorgio, MD, PhD, AGAF

Department of Medical Sciences,

University of Ferrara, Ferrara, Italy

e-mail: deg@aosp.bo.it

Tel.: +39-0532688156

Fax: +39-0532688156

Conflict of interest

The authors declare no conflict of interest

Author contribution

EB, RDeG conceived the study, performed data analysis and wrote the manuscript; AA, FB, VI, performed RNAseq and data analysis; AS, VB, FG, KVB, CE, EB performed immunostaining and western blotting analysis; ML, AI, FT, GZ; AM, MW, GEB, SM provided the clinical cases and tissue biopsies; SM, EB, RDeG, GEB, MS, VS performed critical revision of the manuscript. All authors read the final version of the paper.

Key points

- Primary achalasia is a disorder due to neuronal defects supplying the esophagus leading to altered peristalsis and lack of sphincter relaxation. Nonetheless, the molecular mechanisms involved in this condition are poorly understood.

- Transcriptomic analysis of achalasic tissues identified a dysregulated expression of different genes, in particular c-KIT (downregulated) and INPP4B (upregulated), the latter being linked to Akt pathway regulation.

- Our results unravel novel signaling pathways involved in the neuronal and interstitial cells of Cajal abnormalities in primary achalasia.

Abstract

Background & Aims: Achalasia is a rare motility disorder characterized by myenteric neuron and interstitial cells of Cajal (ICC) abnormalities leading to deranged/absent peristalsis and lack of relaxation of the lower esophageal sphincter. The mechanisms contributing to neuronal and ICC changes in achalasia are only partially understood. Our goal was to identify novel molecular features occurring in patients with primary achalasia.

Methods: Esophageal full-thickness biopsies from 42 (22 females; age range: 16-82 yrs) clinically, radiologically and manometrically characterized patients with primary achalasia were examined and compared to those obtained from ten subjects (controls) undergoing surgery for uncomplicated esophageal cancer (or upper stomach disorders). Tissue RNA extracted from biopsies of cases and controls was used for library preparation and sequencing. Data analysis was performed with the 'edgeR' option of R-Bioconductor. Data were validated by real-time RT-PCR, western blotting and immunohistochemistry.

Key Results: Quantitative transcriptome evaluation and cluster analysis revealed 111 differentially expressed genes, with a $P \leq 10^{-3}$. Nine genes with a $P \leq 10^{-4}$ were further validated. *CYR61*, *CTGF*, *c-KIT*, *DUSP5*, *EGR1* were downregulated, whereas *AKAP6* and *INPP4B* were upregulated in patients *vs* controls. Compared to controls, immunohistochemical analysis revealed a clear increase in INPP4B, whereas c-KIT immunolabeling resulted downregulated. Since INPP4B regulates Akt pathway, we used western blot to show that phospho-Akt was significantly reduced in achalasia patients *vs* controls.

Conclusions & Inferences: The identification of altered gene expression, including *INPP4B*, a regulator of the Akt pathway, highlights novel signaling pathways involved in the neuronal and ICC changes underlying primary achalasia.

Key words: Achalasia, cell signaling, c-KIT, INPP4B, transcriptome.

Introduction

Achalasia is a primary motility disorder of the esophagus occurring at any age, with an estimated annual incidence of approximately 0.03-1 per 100 people and affecting both sexes equally.[1,2] Achalasia can be classified into primary forms (mostly idiopathic), and cases associated with systemic disorders.[3,4] From a pathogenetic stand-point, achalasia is characterized by a predominant loss of inhibitory myenteric neurons with a relative increase of cholinergic motorneurons[5]. Progressively degenerative processes may involve virtually all neurons over time. These neuronal changes result in an increase of the lower esophageal sphincter (LES) tone, which, in conjunction with an altered peristalsis of the esophageal body, represent the manometric correlate of any form of achalasia.[6] Because of these functional abnormalities patients with achalasia complain of dysphagia, regurgitation and chest pain, often severe enough to require either surgery or pneumatic dilatation[7]. Mechanisms leading to esophageal myenteric neurodegeneration and loss include autoimmune responses likely triggered by environmental factors (e.g., neurotropic viruses) in genetically predisposed individuals.[2,3,8] In addition to neurons, abnormalities of interstitial cells of Cajal (ICC), the pace-maker cells of the gastrointestinal tract, were demonstrated in patients with achalasia[9].

The current standard for diagnosing achalasia is high-resolution manometry, although molecular biomarkers would be useful not only for diagnostic purposes, but also to address targeted therapeutic options so far not yet available. Proteomic analysis of sera from patients with achalasia and healthy individuals showed disease-related upregulation of transthyretin (TTR), a carrier of thyroid hormone thyroxine and a retinol-binding protein, associated with familial amyloid polyneuropathy.[10] The

observed upregulation may correlate with the consequent neural degeneration observed in achalasic patients.[11] Other studies demonstrated increased deposits of the complement complex C5b-C9 and IgM within or proximal to ganglion cells of the esophageal myenteric plexus.[12]

Achalasia due to rare genetic abnormalities includes recessive forms with mutations in the neuronal nitric oxide synthase gene, *NOS1*[13], or in *ALADIN* gene[14] (Allgrove syndrome or triple A syndrome, characterized by alacrima, achalasia and adrenal cortex failure; OMIM #231550). Genome-wide and candidate gene association studies have implicated the human leukocyte antigen (HLA) class II system as the underlying genetic predisposing factor in achalasia. In particular, an 8-residues insertion in the cytoplasmic tail of HLA-DQβ1 has been identified as a strong risk factor for achalasia, with a specific geospatial north-south gradient among Europeans.[15] Two amino acid substitutions in the extracellular domain of HLA-DQα1, (lysine 41 encoded by HLA-DQA1*01:03) and of HLA-DQβ1, (glutamic acid 45, encoded by HLA-DQB1*03:01 and HLA-DQB1*03:04) were characterized as independent risk factors for achalasia and patients with the DQA1*0103 and DQB1*0603 alleles have a significantly higher prevalence of anti-myenteric antibodies.[15-20]

Nevertheless, the mechanisms contributing to the observed neuronal and ICC changes in achalasia are still partially understood. The aim of this study was to identify the dysregulated molecular pathways / events occurring in primary (idiopathic) achalasia to provide a molecular signature of primary achalasia.

Materials and Methods

Patients and tissue biopsies

A number of 42 (n= 20 from Italy; n= 22 from Belgium; 22 females; age range: 16-82 yrs) patients with a well-established clinical, radiological and manometric diagnosis of primary achalasia were recruited (Supplementary Table 1A). The included patients were all of Caucasian origin. Each patient underwent surgery and 1-2 tissue samples were obtained via a laparoscopic extramucosal Heller's myotomy extended 4-5 cm along the distal esophagus (i.e., 1-2 cm full-thickness biopsy containing the circular and longitudinal muscle with the associated enteric nervous system). Comparable control tissues were obtained from the corresponding esophageal region of 10 (3 females; age range: 45-87 yrs) controls, who were referred to surgery for uncomplicated esophageal cancer and upper stomach disorders, as reported in Supplementary Table 1B. Margins of all of sampled tissues were free of cancer. Signed informed consent was obtained for each subject enrolled in the study and data handling was performed according to the Helsinki declaration. The study was approved by the local Ethic Committee (study 42/2011/0/Oss protocol #877/211).

RNA extraction

Total RNA was extracted with the RiboPure kit from fresh frozen biopsies stored at -80°C in RNAlater, according to the manufacturer's instruction (Ambion, ThermoFisher Scientific, Waltham, MA, USA). RNA was resuspended in 40 µl of RNase-free water, and quality and quantity of RNA were evaluated on Agilent Bioanalyzer 2100 instrument (Agilent, Santa Clara, CA, USA). 150 ng of RNA was used for each library preparation, according to the TruSeq RNA Sample Prep v2 protocol (Illumina, San Diego, CA, USA). Poly(A)-RNA molecules from 500 ng of total RNA were purified using oligo-dT magnetic beads. Following purification, the mRNA was fragmented and randomly primed for reverse transcription followed by second-strand synthesis to create double-stranded cDNA fragments, that were then

end-repaired and ligated using paired-end sequencing adapters. The products were then amplified to enrich for fragments carrying adapters ligated on both ends, thus creating the final cDNA library. RNAseq was performed on the HiScan SQ platform (Illumina) as 75 bp paired-end.

RNAseq data analysis

Raw paired-end reads obtained by the HiScan SQ were filtered and trimmed with the tool AdapterRemoval (http://code.google.com/p/adapterremoval/) to exclude low quality bases and sequence adapters. Short reads were mapped on human reference genome hg19 (https://genome.ucsc.edu/) with the pipeline Bowtie/Tophat (http://ccb.jhu.edu/software/tophat/index.shtml) and Samtools (http://samtools.sourceforge.net/) was adopted to remove optical/PCR duplicates. Gene expression quantification was performed with the Python package htseq-count (http://www-huber.embl.de/HTSeq/doc/overview.html) using the Ensembl release 72 annotation features (http://www.ensembl.org). The raw counts were normalized with the R-Bioconductor package edger (function calcNormFactors) as "count per million" (cpm). A filter procedure was adopted to analyze only genes with cpm > 3 in at least 2/4 samples. This process allowed to include 9616 genes, that were analyzed with the R-Bioconductor package limma to determine the differentially expressed genes. In particular, the function lmFit was used to fit the linear model, and the function eBayes was adopted to compute the moderate t-statistic. Genes were ranked in order of evidence for differential expression using log2 fold change (log2FC) and *P* value.[21] Multiple Experiment Viewer (MEV) (v4.8.1) was used to perform the analysis in two different ways: unsupervised hierarchical clustering (distance: Manhattan; clustering method: average) and principal component analysis. A total of 111 differentially expressed genes were selected ($P \leq 10^{-3}$) for the evaluation of the functional

classification of biological processes and pathway over-representation, performed with the analytical tools PANTHER13.1 (Protein ANalysis THrough Evolutionary Relationships; http://pantherdb.org) and STRING. PANTHER is tightly integrated with a number of different genomic resources: the InterPro Consortium of protein classification resources, the Quest for Orthologs Consortium and the UniProt Reference Proteome data sets. PANTHER Over-representation tool includes functional annotations directly downloaded from the Gene Ontology (GO) Consortium, in addition to the phylogenetically inferred annotations.[22] Analysis was performed using the option PANTHER Functional Classification and Over-representation Tests, using the PANTHER GO-Slim Biological process and the Fisher's Exact with false discovery rate (FDR) multiple test correction for statistical analysis. Independent analysis to observe protein-protein interaction was performed with STRING, a database of known and predicted protein-protein interactions. The interactions include direct (physical) and indirect (functional) associations; stemming from computational prediction, from knowledge transfer between organisms, and from interactions aggregated from other (primary) databases.[23,24]

Quantitative real-time RT-qPCR

DNase I-treated RNA (200 ng) was used for reverse transcription (RT) with random hexamers using the Multiscribe RT system (ThermoFisher Scientific) at 48°C for 40 min in a final volume of 50 µl. *DNase I*-treated total RNA was obtained from a pool of commercially available fresh frozen tissue biopsies of five controls subjects (single vial purchased from AMSBIO, Abingdon, Oxford, UK; reference code: R1234106-P, lot number B209050, human normal adult esophageal total RNA); the other RNAs were obtained from fresh frozen tissue biopsies as described above.

RT-qPCR was performed with SYBRGreen, 0.5 µM primers, in an ABI 7500 Real-Time PCR System (ThermoFisher Scientific). All target genes were normalized with the endogenous control (beta-actin) using the ΔΔCt comparative method. Primers are available from the Authors on request.

Western blotting

Proteins were extracted from fresh frozen tissue biopsies of esophagus of achalasia patients and controls by sonication using the Diagenode Bioruptor Pico sonicator System (V 1.1) (10 cycles of 30 on/30 off; 20-60 kHz), in a volume of 50 µl of Laemli buffer 1X. A pool of normal esophageal tissues was commercially available (Abcam, Cambridge, UK, reference code ab30243 - Human esophagus normal tissue lysate - total protein), the other tissues analyzed with western blotting were obtained from fresh frozen tissue biopsies of single cases and controls as reported in Supplementary Tables 1A and 1B. Proteins were visualized on Coomassie Blue gel for quality and quantity control. Western blot analysis was performed by SDS gel electrophoresis and transfer onto nitrocellulose membrane, using the TransBlot system (Bio-Rad Laboratories, Segrate, Italy). Primary antibodies used were the following: rabbit anti-INPP4B diluted 1:200 (Abcam); rabbit anti-c-KIT (Abcam) diluted 1:200; mouse anti-vinculin (Sigma-Aldrich, St. Louis, MO, USA) diluted at 1:5000; mouse anti-GAPDH 1:10000 (Abcam); anti p-Akt (Ser473), anti p-Akt (Thr308), anti Akt (Cell Signaling, Leiden, Netherlands), anti β-actin 1:10000 (Sigma-Aldrich). HRPO-conjugated secondary antibodies (Sigma-Aldrich) were diluted 1:35000 in blocking solution. Bands were visualized by the ECL method Supernova (Cyanagen, Bologna, Italy) using the Chemidoc XRS+ Imager and densitometric analysis was performed with Image lab Software (Bio-Rad Laboratories). All western blot analyses were

performed at least in duplicate for each protein extract from each patient and control tissue biopsy.

Immunohistochemistry

Immunohistochemistry was performed on paraffin-embedded adult human esophagus tissues according to protocols validated in our laboratory.[25] Immunohistochemistry analyses and image acquisitions were performed in our laboratory at the University of Bologna. Briefly, tissue sections were treated to remove paraffin embedding by sequential washes in xylene and graded ethanol. Antigen unmasking was performed by heating sections at 95°C in 10 mM Sodium citrate buffer, pH 6.0, for 10 min and subsequent cooling at room temperature for 30 min. To reduce endogenous peroxidases, tissue sections were treated with an ad hoc blocking kit (GeneTex Inc., Irvine, CA, USA) and incubated for 16 h at 4°C with the same primary antibodies used for western blotting, but diluted 1:50. 3,3'-diaminobenzidine staining was performed according to standard protocols (DAB500 IHC Select® kit, Merck Millipore, Darmstadt, Germany). Scores were assigned based on the intensity of DAB staining (0 = no staining; + = 10-50% staining; ++ = 50-90% staining; +++ = ≥90% staining of the areas; all images were acquired at 10x magnification) according to standard pathological assessment.[26] Three expert observers independently evaluated the images (E.B., F.B. and R. De G.), and their analyses were blinded regarding control *vs*. achalasia state. Image capturing of achalasia and control tissues was performed on a Nikon microscope using DS-5M digital camera (Nikon Instruments, Düsseldorf, Germany).

Statistical analysis

Quantitative difference in densitometry of western blots was performed with the Student's t-test option of GraphPad Quickstat calculator; statistical differences for the scores assigned to IHC samples from tissue biopsies was performed with Fisher's Test (4 x 2 contingency table) using the program Vassarstats.

Results

Whole transcriptome analysis via RNAseq

Total RNA extracted from esophageal biopsies of four cases (2F; age range: 30-58 yrs) and four controls (3F; age range: 27-50 yrs) was used for library preparation and sequencing on Illumina HiScan SQ platform. Raw data showing the total amount of reads/library and the mean coverage are reported in Supplementary Table 2, along with the mean coverage for each sample. Quantitative data analysis using Bioconductor from R package identified 111 genes with differential expression between cases and controls at a $P \leq 10^{-3}$ (Table 1). Compared to controls, 77 genes were downregulated and 34 genes were upregulated in the achalasia group. Hierarchical clustering considering the 111 genes was performed using MEV v4.8.1. As shown in the heat map in Figure 1A, a concordant signature of up- and down-regulation expression was evident between cases and controls. Analysis using PANTHER Functional classification test (PANTHER GO Slim Process) led us to functionally map a total of 109 out of the 111 differentially expressed genes to different biological processes, including, amongst others, cell adhesion, biogenesis, developmental, immune and metabolic processes and response to stimuli (http://www.pantherdb.org/chart/pantherChart.jsp?listType=1&filterLevel=1&type=2&chartType=1&save=yes&basketItems=all&zoom=1.25&trackingId=4DCA8C9D00F5C4649E3257CE82CFAC3E) (Figure 1B). PANTHER Over-representation Test

analysis was performed against the *H. sapiens* gene database, showing a set of over-represented biological processes in achalasia, including, amongst others, phosphorylation, the MAPK cascade signaling (including intracellular signal transduction and cell communication), regulation of phosphate metabolism and developmental processes, e.g. cell differentiation and death (FDR< 0.05; Table 2).

Network analysis was performed with STRING using the list of genes (the previously identified 111 genes) reported in Table 1, using the *H. sapiens* database as model organism, and the "whole genome" option as statistical background. A number of 104 out of 111 genes matched the STRING protein database and were included in the analysis (https://string-db.org/cgi/network.pl?taskId=u9O5yLo4Lf2G). Several pathways were identified that showed a functional enrichment for biological processes, such as regulation of development, cell differentiation, angiogenesis and vascular architecture, with significant *P* values reported in Table 3. Many protein-protein interactions converged on c-KIT (Figure 1C).

Among the dysregulated genes in achalasia, those differentially expressed with a significant $P \leq 10^{-4}$ were selected for further investigation, including *CYR61*, *CTGF*, c-*KIT*, *EGR1*, *LIF* and *CD69* (downregulated); and *AKAP6*, and *INPP4B* (overexpressed) (Table 1). To validate the data from whole transcriptome analysis, we performed quantitative real-time RT-qPCR using the total RNA of already sequenced samples (including two patients and one control). For each real-time RT-qPCR, raw data were normalized on a commercial pool of human normal esophagus RNA from fresh frozen tissue biopsies of five individuals (AMSBIO), using the ΔΔCt method. Data reported in Figure 1D show independent technical replicates (same case-control samples, independent retro-transcription and real-time processes). A significant dysregulation of expression was confirmed for *c-KIT* and *INPP4B* (Figure 1D). These

findings prompted us to focus on these two molecular targets, i.e. *c-KIT* and *INPP4B*, which were down- and up-regulated, respectively.

Protein analysis of INPP4B and c-KIT confirmed the RNAseq data

The protein expression of c-KIT and INPP4B was studied by western blotting. In these experiments, control samples included a pool of normal esophageal tissues (Abcam) from five subjects in addition to control tissues obtained from single individual control subjects. Western blotting analysis for each tissue lysate was performed at least in two independent experiments, i.e. technical replicates. Equal amount of proteins was loaded for each sample and intensities were normalized using reference proteins. Representative examples of the protein patterns observed for c-KIT, INPP4B and reference proteins were reported in Figure 2A. Densitometric analysis of western blots was performed as indicated in Figure 2B. All cases and controls included in the western blotting analysis were reported in Supplementary Tables 1A and 1B. c-KIT downregulation was confirmed in tissue biopsies of achalasia patients compared to controls (P= 0.0003, Student's t-test; Figure 2B), whereas INPP4B overexpression was significantly detectable in achalasia patients *vs.* controls (P=0.0381; Student's t-test, Figure 2B).

Immunohistochemistry analysis was performed in order to confirm the western blot data and to determine the cellular localization of the proteins herein identified by western blot. The density of c-KIT immunoreactive cells (mainly with the typical shape of ICC) was lower in achalasia than in controls (Fisher's exact test, P= 0.0005, Figure 3A). Compared to controls, INPP4B immunoreactivity was more intense in achalasia patients. In INPP4B-positive cases, the immunoreactive signal was present in different cells including muscle cells and myenteric ganglia. INPP4B expression in

the normal tissues was very low or virtually absent (Fisher's exact test, *P*= 0.0023; Figure 3B).

Phospho-Akt is down regulated in achalasia

As INPP4B is a negative regulator of Akt signaling, we investigated Akt phosphorylation status. Equal amount of proteins was loaded for each sample and intensities were normalized using reference proteins. Representative examples of the phosphorylation patterns observed for the two phosphorylation sites in Akt (Ser473, and Thr308) were reported in Figure 4A. Densitometric analysis, performed according to our previously published data,[27] revealed that tissue samples from achalasia patients presented a reduced Akt phosphorylation, in particular the phosphorylation at Ser473 was significantly decreased compared to control tissues (*P*=0.0495, Student's t-test; Figure 4B).

Discussion

Primary achalasia causes significant impairment of esophageal motility leading to symptom generation and overall reduced patients' quality of life. This esophageal dysmotility of the esophagus has a complex etio-pathogenesis. Recent findings indicate that both an inflammatory / immune-mediated insult, as exhibited by myenteric ganglionitis (likely driven by neurotropic, e.g. herpes, virus infection)[28] and circulating anti-neuronal antibodies, play a pathogenetic role. A genetic predisposition conferred by HLA genetic background[20] can contribute to neural abnormalities underlying achalasia. A predominant genetic component has been identified in well-defined conditions such as 'triple A' (also referred to Allgrove's syndrome), where mutations in the ALADIN gene[14] were found in familial clusters. Other data derive

from *NOS1*, which encodes for the neuronal nitric oxide synthase. A stop codon mutation of this gene has been reported in a family where two children manifested a very severe clinical phenotype dominated by achalasia.[13] Nevertheless, in the majority of cases the factors causing achalasia remain to be elucidated. As a consequence, the available therapeutic approaches are far from targeting the actual mechanisms leading to the neural impairment recognized to be the *primum movens* of this severe esophageal disorder. New understanding of achalasia, involving a deeper knowledge of the attendant molecular mechanisms, should aim to a better patient management and stop the disease at early stages. Therefore, the present study attempted to decipher the altered molecular pathways in patients with achalasia. We strategically used esophageal tissues from achalasic patients and examined gene expression via whole transcriptome analysis in order to provide novel targets for a therapeutic approach. From the RNAseq data we detected 111 genes with an altered expression. Functional classification and over-representation analysis of the biological processes, where these genes mapped, was performed with two different bioinformatic tools, PANTHER and STRING. Results showed a significant over-representation of phosphorylation processes, intracellular signaling, cell communication and development /differentiation processes, including cell death. These data suggest that an imbalance of cell growth/survival *vs.* cell death may cause the defects observed in the achalasia tissues, not only in term of neuron loss, but also as an overall tissue degeneration. Notably, in a recent study, Palmieri et al. performed transcriptome analysis on tissues of primary achalasia patients and identified a significant enrichment of neuro-muscular and neuro-immune processes. These data support the concept that achalasia results from degenerative alterations / loss of myenteric

neurons mainly evoked by a chronic inflammatory infiltrate targeting the myenteric plexus.[29]

Among the genes with significant dysregulation, we confirmed by real-time qPCR *c-KIT* downregulation and *INPP4B* upregulation, respectively. *c-KIT* significant downregulation, validated both via western blot and immunohistochemistry, confirms and expands previously reported data showing a loss of ICC network in tissues of patients with primary achalasia.[9] Our data highlighting a significant decrease of c-KIT expression in human achalasia support the concept that stem cell factor, the major ligand to c-KIT, cannot mediate ICC maintenance and survival. Although we did not look into specific apoptotic mechanisms, it is likely that a programmed cell death can involve ICC in achalasia.[30] Since ICC play a role in esophageal motility, their depletion can contribute to the deranged mechanisms leading to altered motility in achalasia.[31]

The second gene for which we were able to confirm an altered expression at the protein level is INPP4B, encoding for inositol polyphosphate-4-phosphatase type II B, a negative regulator of Akt.[32,33] The expression of this phosphatase was upregulated in many cell types in tissues from achalasic patients, indicating a general increase in inhibitory signals for cell survival, a mechanism stimulated by Akt-dependent pathways.[32] Thus, an INPP4B increased expression can be correlated to the enrichment in genes involved in cell death. Notably, in achalasia tissues we observed a decrease in the phosphorylation of the Ser473 in Akt, which is a key phosphorylation step for its activation and function. Therefore, it may be postulated that in achalasia the altered molecular signaling led to an overall impaired cell survival, which, in the long term, generates a permanent tissue damage. Thus, one can assume that also ICCs, in addition to neurons, can be affected. Since many studies

have investigated the Akt / INPP4B pathway as a potential "druggable" route to block tumor proliferation,[33,34] the development of *ad hoc* molecules may become relevant for patients with primary achalasia.

In conclusion, our study highlights the altered expression of two distinct genes, i.e. c-KIT and INPP4B down- and up-regulation, in patients with primary achalasia. Our results may provide a basis for future research aimed at investigating novel therapeutic targets for patients with primary achalasia.

Acknowledgements

The authors wish to thank all patients that participated in the study. We thank Drs. A. Gori, and V. Bertakis and Ms. G. Galiazzo for technical help.

References

1. Boeckxstaens GE, Zaninotto G, Richter JE. Achalasia. Lancet 2014;383:83-93.

2. Moonen A, Boeckxstaens G. Current diagnosis and management of achalasia. J Clin Gastroenterology 2014;48:484-90.

3. Kahrilas PJ, Boeckxstaens G. The spectrum of achalasia: lessons from studies of pathophysiology and high resolution manometry. Gastroenterology 2013;145:954-65.

4. Di Nardo G, Tullio-Pelet A, Annese V, et al. Idiopathic achalasia is not allelic to alacrima achalasia adrenal insufficiency syndrome at the ALADIN locus. Dig Liver Dis 2005;37:312-5.

5. Goldblum, JR, Rice, TW, Richter JE. Histopathologic features in esophagomyotomy specimens from patients with achalasia. Gastroenterology 1996;111:648-54.

6. Roman S, Gyawali CP, Xiao Y, Pandolfino JE, Kahrilas PJ. The Chicago classification of motility disorders: an update. Gastrointest Endosc Clin North Am 2014;24:545-61.

7. Boeckxstaens GE, Annese V, des Varannes SB, et al. European Achalasia Trial Investigators. Pneumatic dilation versus laparoscopic Heller's myotomy for idiopathic achalasia. N Engl J Med 2011;364:1807-16.

8. Ates F, Vaezi MF. The Pathogenesis and management of achalasia: Current status and future directions. Gut Liver 2015;9:449-63.

9. Gockel I, Bohl JR, Eckardt VF, Junginger T. Reduction of interstitial cells of Cajal (ICC) associated with neuronal nitric oxide synthase (n-NOS) in patients with achalasia. Am J Gastroenterol 2008;103:856-64.

10. Saraiva MJM, Birken S, Costa PP, Goodman DS. Amyloid fibril protein in familial amyloidotic polyneuropathy, Portuguese type: definition of molecular abnormality in transthyretin (prealbumin). J Clin Invest 1984;74:104-19.

11. Sodikoff JB, Lo AA, Shetuni BB, Kahrilas PJ, Yang GY, Pandolfino JE. Histopathologic patterns among achalasia subtypes. Neurogastroenterol Motil 2016;28:139-45.

12. Storch WB, Eckardt VF, Junginger T. Complement components and terminal complement complex in oesophageal smooth muscle of patients with achalasia. Cell Mol Biol (Noisy-le-grand) 2002;48:247-52.

13. Shteyer E, Edvardson S, Wynia-Smith SL, et al. Truncating mutation in the nitric oxide synthase 1 gene is associated with infantile achalasia. Gastroenterology

2015;148:533-36.

14. Tullio-Pelet A, Salomon R, Hadj-Rabia S, et al. Mutant WD-repeat protein in triple-A syndrome. Nat Genet 2000;26:332-5.

15. Becker J, Haas SL, Mokrowiecka A, et al. The HLA-DQβ1 insertion is a strong achalasia risk factor and displays a geospatial north-south gradient among Europeans. Eur J Hum Genet 2016;24:1228-31.

16. Verne GN, Sallustio JE, Eaker EY. Anti-myenteric neuronal antibodies in patients with achalasia. A prospective study. Dig Dis Sci 1997;42:307-13.

17. Ruiz-de-León A, Mendoza J, Sevilla-Mantilla C, et al. Myenteric antiplexus antibodies and class II HLA in achalasia. Dig Dis Sci 2002;47:15-19.

18. Latiano A, De Giorgio R, Volta U, et al. HLA and enteric antineuronal antibodies in patients with achalasia. Neurogastroenterol Motil 2006;18:520-25.

19. De la Concha EG, Fernandez-Arquero M, Mendoza JL, et al. Contribution of HLA class II genes to susceptibility in achalasia. Tissue Antigens 1998;52:381-84.

20. Gockel I, Becker J, Wouters MM, et al. Common variants in the HLA-DQ region confer susceptibility to idiopathic achalasia. Nat Genet 2014;46:901-4.

21. Nannini M, Astolfi A, Urbini M, et al. Integrated genomic study of quadruple-WT GIST (KIT/PDGFRA/SDH/RAS pathway wild-type GIST). BMC Cancer. 2014;14:685.

22. Huang X, Muruganujan A, Tang H, et al. PANTHER version 11: expanded annotation data from Gene Ontology and Reactome pathways, and data analysis tool enhancements. Nucleic Acids Research, 2017;45:D183–9.

23. Szklarczyk D, Morris JH, Cook H, et al. The STRING database in 2017: quality-controlled protein-protein association networks, made broadly accessible. Nucleic Acids Res. 2017; 45: D362–D368.

24. Szklarczyk D, Franceschini A, Wyder S, et al. STRING v10: protein-protein interaction networks, integrated over the tree of life. Nucleic Acids Res. 2015 Jan; 43:D447-52.

25. Bonora E, Bianco F, Cordeddu L, et al. Mutations in RAD21 disrupt regulation of APOB in patients with chronic intestinal pseudo-obstruction. Gastroenterology 2015;148:771-82.e11.

26. Couch G, Redman JE, Wernisch L, Newton R, et al. The Discovery and Validation of Biomarkers for the Diagnosis of Esophageal Squamous Dysplasia and Squamous. Cancer Prev Res (Phila). 2016;9:558-66.

27. Buontempo F, Orsini E, Lonetti A, et al. Synergistic cytotoxic effects of bortezomib and CK2 inhibitor CX-4945 in acute lymphoblastic leukemia: turning off the prosurvival ER chaperone BIP/Grp78 and turning on the pro-apoptotic NF-κB. Oncotarget. 2016;7:1323-40.

28. Moonen A, Boeckxstaens GE. Finding the right treatment for achalasia treatment: Risks, efficacy, complications. Curr Treat Options Gastroenterol 2016;14:420-28.

29. Palmieri O, Mazza T, Merla A, et al. Gene expression of muscular and neuronal pathways is cooperatively dysregulated in patients with idiopathic achalasia. Sci Rep 2016;6:31549.

30. Gibbons SJ, De Giorgio R, Faussone Pellegrini MS, et al. Apoptotic cell death of human interstitial cells of Cajal. Neurogastroenterol Motil 2009;21:85-93.

31. Farrugia G. Histologic changes in diabetic gastroparesis. Gastroenterol Clin North Am. 2015;44:31-8.

32. Rodgers SJ, Ferguson DT, Mitchell CA, Ooms LM. Regulation of PI3K effector signalling in cancer by the phosphoinositide phosphatases. Biosci Rep 2017;10:37(1).

33. Chew CL, Chen M, Pandolfi PP. Endosome and INPP4B. Oncotarget 2016;7:5-6.

34. Li Chew C, Lunardi A, Gulluni F, et al. In vivo role of INPP4B in tumor and metastasis suppression through regulation of PI3K-AKT signaling at endosomes. Cancer Discov 2015;5:740-51.

Table 1. Genes differentially expressed in achalasia.

Genes overexpressed in achalasia are labeled in red. Green shadowed area indicates the genes with a $P \leq 10^{-4}$.

ENSEMBL transcript ID	GENE name	log2 Fold Change	*P* value
ENST00000451137	*CYR61*	*-2.99*	*9.71E-06*
ENST00000367976	*CTGF*	*-2.74*	*1.19E-05*
ENST00000513000	*INPP4B*	*1.63*	*1.42E-04*
ENST00000288135	*KIT*	*-1.48*	*4.17E-04*
ENST00000249075	*LIF*	*-2.40*	*4.23E-04*
ENST00000239938	*EGR1*	*-1.95*	*4.65E-04*
ENST00000228434	*CD69*	*-3.84*	*4.94E-04*
ENST00000280979	*AKAP6*	*1.63*	*7.28E-04*
ENST00000296464	*HSPA4L*	*1.07*	*8.99E-04*
ENST00000319653	FMN2	2.03	1.11E-03
ENST00000517956	FBXO32	1.26	1.12E-03
ENST00000265634	NPTX2	-1.88	1.20E-03
ENST00000550683	ACVRL1	-1.14	1.25E-03
ENST00000378827	BMP2	-1.99	1.51E-03
ENST00000371852	CH25H	-3.06	1.56E-03
ENST00000284669	KLHL41	2.43	1.58E-03
ENST00000436924	BRE	2.70	1.60E-03
ENST00000561981	FRRS1L	1.51	1.62E-03
ENST00000307792	SEMA3E	1.07	1.66E-03
ENST00000330871	SOCS3	-2.47	2.07E-03
ENST00000331569	ZNF703	1.18	2.30E-03
ENST00000305988	ADRB2	-1.41	2.47E-03
ENST00000420022	ADM5	-1.80	2.58E-03
ENST00000297316	SOX17	-1.82	2.76E-03
ENST00000252590	PLVAP	-1.29	2.77E-03
ENST00000256103	PMP2	-2.28	2.87E-03
ENST00000329099	FAM101B	-1.32	3.11E-03
ENST00000287814	TIMP4	-1.25	3.12E-03
ENST00000300177	GREM1	-2.58	3.29E-03
ENST00000485685	GGNBP2	-1.78	3.40E-03
ENST00000365328	RN7SK	-1.61	3.41E-03
ENST00000284878	CXADR	2.20	3.47E-03
ENST00000296046	CPA3	-1.76	3.52E-03
ENST00000302754	JUNB	-1.73	3.74E-03
ENST00000437551	PAX8-AS1	1.36	3.74E-03
ENST00000322507	COL12A1	-1.10	3.80E-03
ENST00000307637	C3AR1	-1.86	3.82E-03
ENST00000340695	SCXA	2.40	3.88E-03
ENST00000322954	UACA	0.94	3.89E-03

ENST00000055682	KIAA2022	1.00	3.92E-03
ENST00000379374	PHEX	-3.10	3.98E-03
ENST00000357949	SERTAD1	-1.45	4.02E-03
ENST00000230990	HBEGF	-2.36	4.08E-03
ENST00000359534	KCNK5	-2.25	4.16E-03
ENST00000224605	GDF10	-1.64	4.17E-03
ENST00000396184	PDE1C	1.02	4.32E-03
ENST00000373509	PIM1	-2.29	4.33E-03
ENST00000408965	CEBPD	-1.45	4.59E-03
ENST00000267984	MESDC1	-1.17	4.82E-03
ENST00000329608	CSF1	-1.16	4.92E-03
ENST00000344120	SPRY4	-1.18	5.13E-03
ENST00000395076	PPM1A	0.85	5.16E-03
ENST00000350896	MSR1	-1.37	5.21E-03
ENST00000366667	AGT	-1.68	5.22E-03
ENST00000263370	ITPKC	-1.75	5.24E-03
ENST00000259989	FGFBP2	-1.75	5.24E-03
ENST00000311922	TRIB1	-2.74	5.24E-03
ENST00000608521	MIR663A	2.80	5.25E-03
ENST00000377103	THBD	-2.31	5.27E-03
ENST00000422542	AC005682,5	-1.34	5.32E-03
ENST00000396037	ST8SIA1	1.75	5.39E-03
ENST00000264805	PDE5A	2.61	5.58E-03
ENST00000400546	NCAM2	-1.27	5.65E-03
ENST00000369026	MCL1	-1.16	6.00E-03
ENST00000515896	RNA5-8SP6	1.12	6.20E-03
ENST00000399799	ROCK1	0.96	6.23E-03
ENST00000273153	CSRNP1	-1.74	6.25E-03
ENST00000244221	PAIP2B	1.09	6.25E-03
ENST00000376414	GPR183	-1.77	6.40E-03
ENST00000500741	DYNLL1-AS1	1.16	6.57E-03
ENST00000308086	THAP2	0.91	6.67E-03
ENST00000274063	SFRP2	-1.92	6.68E-03
ENST00000290551	BTG2	-1.53	6.72E-03
ENST00000380392	C2CD4B	-2.57	6.78E-03
ENST00000410087	CERKL	-1.36	6.83E-03
ENST00000367558	RGS16	-2.28	7.09E-03
ENST00000256257	RNF122	-1.65	7.10E-03
ENST00000367511	FAM129A	0.64	7.12E-03
ENST00000592790	VMP1	-2.93	7.17E-03
ENST00000323040	GPR4	-1.97	7.27E-03
ENST00000307851	HAVCR2	-1.68	7.40E-03
ENST00000324559	ANO5	0.96	7.62E-03
ENST00000328041	SLC24A3	-1.35	7.63E-03
ENST00000311734	IL1RL1	-3.50	7.72E-03
ENST00000373313	MAFB	-1.65	8.05E-03

ENST00000382723	MSX1	-2.11	8.32E-03
ENST00000379731	B4GALT1	-1.49	8.33E-03
ENST00000329399	PDLIM1	-1.46	8.42E-03
ENST00000369583	DUSP5	-1.58	8.43E-03
ENST00000332029	SOCS1	-1.69	8.47E-03
ENST00000441535	FMO2	-1.27	8.55E-03
ENST00000256951	EMP1	-2.33	8.71E-03
ENST00000239223	DUSP1	-1.08	8.75E-03
ENST00000330106	CEND1	-2.85	8.84E-03
ENST00000498165	PPM1L	1.08	8.87E-03
ENST00000506002	MTND6P4	1.03	8.91E-03
ENST00000244050	SNAI1	-1.59	8.93E-03
ENST00000380874	FOXC1	-1.77	8.94E-03
ENST00000396073	ENAM	2.83	9.03E-03
ENST00000272928	ACKR3	-1.31	9.04E-03
ENST00000379359	RGCC	-1.11	9.22E-03
ENST00000333926	CISD1	0.80	9.30E-03
ENST00000367996	ADAMTS4	-4.18	9.37E-03
ENST00000380079	STEAP4	-2.07	9.38E-03
ENST00000413366	PRKCA	1.03	9.39E-03
ENST00000215794	USP18	-1.45	9.57E-03
ENST00000305352	S1PR1	-1.27	9.74E-03
ENST00000306065	ANKRD27	0.67	9.81E-03
ENST00000222390	HGF	-2.02	9.83E-03
ENST00000358432	EPHA2	-1.13	9.85E-03
ENST00000270001	ZFP14	0.88	9.89E-03

535

536

Table 2. Output of PANTHER Over-representation test of biological processes enriched for the genes differentially expressed in achalasia tissues, compared to H. sapiens gene PANTHER database.

PANTHER GO Slim Biological process	*H. sapiens*	Achalasia	Expected	Fold enrichment	Hierarchy (+/-)	raw *P* value	False Discovery Rate
Protein phosphorylation	81	4	.42	9.53	+	9.80e-04	3.99e-02
MAPK cascade	340	9	1.76	5.11	+	8.19e-05	6.66e-03
• intracellular signal transduction	1071	17	5.55	3.06	+	4.05e-05	4.94e-03
• signal transduction	2318	24	12.01	2.00	+	1.01e-03	3.54e-02
• Cell communication	2686	26	13.91	1.87	+	1.39e-03	3.76e-02
Regulation of catalytic activity	359	9	1.86	4.84	+	1.22e-04	7.47e-03
• regulation of molecular function	441	9	2.28	3.94	+	5.38e-04	2.62e-02
Regulation of phosphate metabolic process	537	12	2.78	4.31	+	2.64e-05	6.44e-03
Developmental process	1501	18	7.78	2.32	+	1.03e-03	3.13e-02

Only results with False Discovery Rate<0.05 are reported in the table.

Table 3: Output of STRING (protein-protein interaction and biological processes) for genes differentially regulated from whole transcriptome analysis of achalasia tissues.

	Pathway ID and description	Count in gene set	False Discovery Rate *P* values
Biological Process (GO)	GO 0051094 positive regulation of developmental process	29	1.97e-10
	GO 1901342 regulation of vascular development	15	8.62e-10
	GO 0045597 positive regulation of cell differentiation	24	1.44e-09
	GO 004565 regulation of angiogenesis	14	2.7e-09
	GO 2000026 regulation of multicellular organismal development	31	3.31e-09
Molecular function (GO)	GO 0001228 transcriptional activator activity, RNA polymerase II transcription regulatory region sequence-specific binding	9	0.0483
	GO 0005515 protein binding	40	0.0483
	GO 0008083 growth factor activity	3	0.0483
Cellular component (GO)	GO 005615 extracellular space	20	0.00342
	GO 0009986 cell surface	14	0.00552

Statistical background selected for the enrichment analysis set to "whole genome".

Figure Legends

Figure 1. Differentially expressed genes in achalasia tissue. (A) Heat map showing the concordant differential expression observed in the tissues from achalasia patients compared to controls (for the genes reported in Table 1). Elaborated with MeV v4.8.1. (B) Biological processes of genes (GO-Slim Biological processes) differentially expressed in achalasia, as identified by PANTHER Functional Classification analysis. (C) Graphical output of significantly enriched protein-protein interactions determined with STRING analysis, showing the results of the 104 out of 111 dysregulated genes in achalasia, compared with data present in the STRING databases. The different colors in the figure inset identify the evidence for the different interactions (known; predicted; identified with other means, such as co-expression, data mining, and protein homology). The red square indicates c-KIT. (D) Real-time qRT-PCR data for *c-KIT* and *INPP4B*. Data from case and control tissue biopsies were normalized on a commercial pool of control tissue biopsies from esophagus. Student's t-test was performed and *P* values are indicated. Bars indicate standard deviations.

Figure 2. Western blot analysis of differentially expressed genes. (A) Example of the protein expression profiles in achalasia tissues compared to control samples for c-KIT and INPP4B. Western blotting was repeated in at least two independent experiments. (B) Densitometric analysis of the relative intensities for c-KIT and INPP4B. Quantitative data (mean values ± standard deviation) from different experiments obtained from each individual were compared using Student's t-test for statistical analysis. For each sample, densitometric values were normalized on reference protein (vinculin). All experiments were carried out at least twice. Bars indicated standard deviations. *P* values are indicated in the graphs.

Figure 3. Immunostaining for c-KIT (A) and INPP4B (B). (A) Examples of the expression pattern for c-KIT in tissue biopsies from control (left) and achalasia patients (right). Arrows indicate the positive staining for c-KIT. c-KIT staining color histograms of controls (n=6) and cases (n=18) represent the number of samples assessed according to the semi-quantitative score. c-KIT immunolabeling differences in cases *vs.* controls were assessed by Fisher's exact test. (B) Examples of the expression pattern for INPP4B in tissue biopsies from control (left) and achalasia patients (right). INPP4B staining color histograms of controls (n=6) and cases (n=22) represent the number of samples assessed according to the semi-quantitative score. INPP4B immunolabeling differences in cases vs. controls were assessed by Fisher's exact test. Scale bars are 100µm as indicated.

Figure 4. Phospho-Akt is down regulated in achalasia. (A) Example of the protein expression profiles in achalasia tissues compared to control samples of phospho-Akt (Ser473; Thr308) and total Akt. (B) Quantitative data (mean values ± standard deviation) from different experiments (performed in duplicate) obtained from each individual were compared using Student's t-test. For each sample, densitometric values were normalized on reference protein (β-actin). The significantly different relative phospho-Akt (Ser473) levels comparing achalasia vs. control tissues, were reported in the histogram (P=0.0495, Student's t-test). Bars indicate standard deviations.

INPP4B overexpression and *c-KIT* downregulation in human achalasia

Running title: *INPP4B and c-KIT dysregulation in achalasia*

Elena Bonora[1], Francesca Bianco[1,2], Agnese Stanzani[1,2], Fiorella Giancola[1,2,3], Annalisa Astolfi[4], Valentina Indio[4], Cecilia Evangelisti[5], Alberto Maria Martelli[5], Elisa Boschetti[1,3], Marialuisa Lugaresi[1], Alexandros Ioannou[1], Francesco Torresan[6], Vincenzo Stanghellini[1], Paolo Clavenzani[2], Marco Seri[1], An Moonen[7], Kim Van Beek[7], Mira Wouters[7], Guy E. Boeckxstaens[7], Giovanni Zaninotto[8], Sandro Mattioli[1] and Roberto De Giorgio[9]

[1] Department of Medical and Surgical Sciences, DIMEC, University of Bologna and St. Orsola-Malpighi Hospital, Bologna, Italy.

[2] Department of Medical and Veterinary Sciences, DIMEVET, University of Bologna, Bologna, Italy.

[3] Centro di Ricerca Biomedica Applicata, St.Orsola-Malpighi Hospital, Bologna, Italy

[4] Interdepartmental Center for Cancer Research "G. Prodi" (CIRC), University of Bologna, Bologna, Italy.

[5] Department of Experimental Medicine, DIMES, University of Bologna, Bologna, Italy.

[6] Department of Digestive System, St. Orsola-Malpighi Hospital, Bologna, Italy.

[7] Translational Research in GastroIntestinal Disorders (TARGID), Department of Clinical and Experimental Medicine, KU Leuven University, Belgium.

[8] Division of Surgery, Imperial College London, London, United Kingdom.

[9] Department of Medical Sciences, Nuovo Arcispedale S.Anna at Cona (Ferrara), University of Ferrara, Italy.

Funding

FB is recipient of a Telethon fellowship. This work was supported by grant GGP15171 from Fondazione Telethon and University of Bologna (RFO funds) to EB and RDeG. RDeG received research grants from Fondazione Del Monte of Bologna and Ravenna. The funding bodies did not influence the content of this article.

Abbreviations

CPM - count per million, GO - gene ontology, LES - lower esophageal sphincter, MEV - multiple experiment viewer, ICC - interstitial cells of Cajal, INPP4B - inositol polyphosphate-4-phosphatase, type II B.

Correspondence address:

Roberto De Giorgio, MD, PhD, AGAF

Department of Medical Sciences,

University of Ferrara, Ferrara, Italy

e-mail: deg@aosp.bo.it

Tel.: +39-0532688156

Fax: +39-0532688156

Conflict of interest

The authors declare no conflict of interest

Author contribution

EB, RDeG conceived the study, performed data analysis and wrote the manuscript; AA, FB, VI, performed RNAseq and data analysis; AS, VB, FG, KVB, CE, EB performed immunostaining and western blotting analysis; ML, AI, FT, GZ; AM, MW, GEB, SM provided the clinical cases and tissue biopsies; SM, EB, RDeG, GEB, MS, VS performed critical revision of the manuscript. All authors read the final version of the paper.

Key points

- Primary achalasia is a disorder due to neuronal defects supplying the esophagus leading to altered peristalsis and lack of sphincter relaxation. Nonetheless, the molecular mechanisms involved in this condition are poorly understood.

- Transcriptomic analysis of achalasic tissues identified a dysregulated expression of different genes, in particular c-KIT (downregulated) and INPP4B (upregulated), the latter being linked to Akt pathway regulation.

- Our results unravel novel signaling pathways involved in the neuronal and interstitial cells of Cajal abnormalities in primary achalasia.

Abstract

Background & Aims: Achalasia is a rare motility disorder characterized by myenteric neuron and interstitial cells of Cajal (ICC) abnormalities leading to deranged/absent peristalsis and lack of relaxation of the lower esophageal sphincter. The mechanisms contributing to neuronal and ICC changes in achalasia are only partially understood. Our goal was to identify novel molecular features occurring in patients with primary achalasia.

Methods: Esophageal full-thickness biopsies from 42 (22 females; age range: 16-82 yrs) clinically, radiologically and manometrically characterized patients with primary achalasia were examined and compared to those obtained from ten subjects (controls) undergoing surgery for uncomplicated esophageal cancer (or upper stomach disorders). Tissue RNA extracted from biopsies of cases and controls was used for library preparation and sequencing. Data analysis was performed with the 'edgeR' option of R-Bioconductor. Data were validated by real-time RT-PCR, western blotting and immunohistochemistry.

Key Results: Quantitative transcriptome evaluation and cluster analysis revealed 111 differentially expressed genes, with a $P \leq 10^{-3}$. Nine genes with a $P \leq 10^{-4}$ were further validated. *CYR61*, *CTGF*, *c-KIT*, *DUSP5*, *EGR1* were downregulated, whereas *AKAP6* and *INPP4B* were upregulated in patients *vs* controls. Compared to controls, immunohistochemical analysis revealed a clear increase in INPP4B, whereas c-KIT immunolabeling resulted downregulated. Since INPP4B regulates Akt pathway, we used western blot to show that phospho-Akt was significantly reduced in achalasia patients *vs* controls.

Conclusions & Inferences: The identification of altered gene expression, including *INPP4B*, a regulator of the Akt pathway, highlights novel signaling pathways involved in the neuronal and ICC changes underlying primary achalasia.

Key words: Achalasia, cell signaling, c-KIT, INPP4B, transcriptome.

Introduction

Achalasia is a primary motility disorder of the esophagus occurring at any age, with an estimated annual incidence of approximately 0.03-1 per 100 people and affecting both sexes equally.[1,2] Achalasia can be classified into primary forms (mostly idiopathic), and cases associated with systemic disorders.[3,4] From a pathogenetic stand-point, achalasia is characterized by a predominant loss of inhibitory myenteric neurons with a relative increase of cholinergic motorneurons[5]. Progressively degenerative processes may involve virtually all neurons over time. These neuronal changes result in an increase of the lower esophageal sphincter (LES) tone, which, in conjunction with an altered peristalsis of the esophageal body, represent the manometric correlate of any form of achalasia.[6] Because of these functional abnormalities patients with achalasia complain of dysphagia, regurgitation and chest pain, often severe enough to require either surgery or pneumatic dilatation[7]. Mechanisms leading to esophageal myenteric neurodegeneration and loss include autoimmune responses likely triggered by environmental factors (e.g., neurotropic viruses) in genetically predisposed individuals.[2,3,8] In addition to neurons, abnormalities of interstitial cells of Cajal (ICC), the pace-maker cells of the gastrointestinal tract, were demonstrated in patients with achalasia[9].

The current standard for diagnosing achalasia is high-resolution manometry, although molecular biomarkers would be useful not only for diagnostic purposes, but also to address targeted therapeutic options so far not yet available. Proteomic analysis of sera from patients with achalasia and healthy individuals showed disease-related upregulation of transthyretin (TTR), a carrier of thyroid hormone thyroxine and a retinol-binding protein, associated with familial amyloid polyneuropathy.[10] The

observed upregulation may correlate with the consequent neural degeneration observed in achalasic patients.[11] Other studies demonstrated increased deposits of the complement complex C5b-C9 and IgM within or proximal to ganglion cells of the esophageal myenteric plexus.[12]

Achalasia due to rare genetic abnormalities includes recessive forms with mutations in the neuronal nitric oxide synthase gene, *NOS1*[13], or in *ALADIN* gene[14] (Allgrove syndrome or triple A syndrome, characterized by alacrima, achalasia and adrenal cortex failure; OMIM #231550). Genome-wide and candidate gene association studies have implicated the human leukocyte antigen (HLA) class II system as the underlying genetic predisposing factor in achalasia. In particular, an 8-residues insertion in the cytoplasmic tail of HLA-DQβ1 has been identified as a strong risk factor for achalasia, with a specific geospatial north-south gradient among Europeans.[15] Two amino acid substitutions in the extracellular domain of HLA-DQα1, (lysine 41 encoded by HLA-DQA1*01:03) and of HLA-DQβ1, (glutamic acid 45, encoded by HLA-DQB1*03:01 and HLA-DQB1*03:04) were characterized as independent risk factors for achalasia and patients with the DQA1*0103 and DQB1*0603 alleles have a significantly higher prevalence of anti-myenteric antibodies.[15-20]

Nevertheless, the mechanisms contributing to the observed neuronal and ICC changes in achalasia are still partially understood. The aim of this study was to identify the dysregulated molecular pathways / events occurring in primary (idiopathic) achalasia to provide a molecular signature of primary achalasia.

Materials and Methods

Patients and tissue biopsies

A number of 42 (n= 20 from Italy; n= 22 from Belgium; 22 females; age range: 16-82 yrs) patients with a well-established clinical, radiological and manometric diagnosis of primary achalasia were recruited (Supplementary Table 1A). The included patients were all of Caucasian origin. Each patient underwent surgery and 1-2 tissue samples were obtained via a laparoscopic extramucosal Heller's myotomy extended 4-5 cm along the distal esophagus (i.e., 1-2 cm full-thickness biopsy containing the circular and longitudinal muscle with the associated enteric nervous system). Comparable control tissues were obtained from the corresponding esophageal region of 10 (3 females; age range: 45-87 yrs) controls, who were referred to surgery for uncomplicated esophageal cancer and upper stomach disorders, as reported in Supplementary Table 1B. Margins of all of sampled tissues were free of cancer. Signed informed consent was obtained for each subject enrolled in the study and data handling was performed according to the Helsinki declaration. The study was approved by the local Ethic Committee (study 42/2011/0/Oss protocol #877/211).

RNA extraction

Total RNA was extracted with the RiboPure kit from fresh frozen biopsies stored at -80°C in RNAlater, according to the manufacturer's instruction (Ambion, ThermoFisher Scientific, Waltham, MA, USA). RNA was resuspended in 40 µl of RNase-free water, and quality and quantity of RNA were evaluated on Agilent Bioanalyzer 2100 instrument (Agilent, Santa Clara, CA, USA). 150 ng of RNA was used for each library preparation, according to the TruSeq RNA Sample Prep v2 protocol (Illumina, San Diego, CA, USA). Poly(A)-RNA molecules from 500 ng of total RNA were purified using oligo-dT magnetic beads. Following purification, the mRNA was fragmented and randomly primed for reverse transcription followed by second-strand synthesis to create double-stranded cDNA fragments, that were then

end-repaired and ligated using paired-end sequencing adapters. The products were then amplified to enrich for fragments carrying adapters ligated on both ends, thus creating the final cDNA library. RNAseq was performed on the HiScan SQ platform (Illumina) as 75 bp paired-end.

RNAseq data analysis

Raw paired-end reads obtained by the HiScan SQ were filtered and trimmed with the tool AdapterRemoval (http://code.google.com/p/adapterremoval/) to exclude low quality bases and sequence adapters. Short reads were mapped on human reference genome hg19 (https://genome.ucsc.edu/) with the pipeline Bowtie/Tophat (http://ccb.jhu.edu/software/tophat/index.shtml) and Samtools (http://samtools.sourceforge.net/) was adopted to remove optical/PCR duplicates. Gene expression quantification was performed with the Python package htseq-count (http://www-huber.embl.de/HTSeq/doc/overview.html) using the Ensembl release 72 annotation features (http://www.ensembl.org). The raw counts were normalized with the R-Bioconductor package edger (function calcNormFactors) as "count per million" (cpm). A filter procedure was adopted to analyze only genes with cpm > 3 in at least 2/4 samples. This process allowed to include 9616 genes, that were analyzed with the R-Bioconductor package limma to determine the differentially expressed genes. In particular, the function lmFit was used to fit the linear model, and the function eBayes was adopted to compute the moderate t-statistic. Genes were ranked in order of evidence for differential expression using log2 fold change (log2FC) and *P* value.[21] Multiple Experiment Viewer (MEV) (v4.8.1) was used to perform the analysis in two different ways: unsupervised hierarchical clustering (distance: Manhattan; clustering method: average) and principal component analysis. A total of 111 differentially expressed genes were selected ($P \leq 10^{-3}$) for the evaluation of the functional

classification of biological processes and pathway over-representation, performed with the analytical tools PANTHER13.1 (Protein ANalysis THrough Evolutionary Relationships; http://pantherdb.org) and STRING. PANTHER is tightly integrated with a number of different genomic resources: the InterPro Consortium of protein classification resources, the Quest for Orthologs Consortium and the UniProt Reference Proteome data sets. PANTHER Over-representation tool includes functional annotations directly downloaded from the Gene Ontology (GO) Consortium, in addition to the phylogenetically inferred annotations.[22] Analysis was performed using the option PANTHER Functional Classification and Over-representation Tests, using the PANTHER GO-Slim Biological process and the Fisher's Exact with false discovery rate (FDR) multiple test correction for statistical analysis. Independent analysis to observe protein-protein interaction was performed with STRING, a database of known and predicted protein-protein interactions. The interactions include direct (physical) and indirect (functional) associations; stemming from computational prediction, from knowledge transfer between organisms, and from interactions aggregated from other (primary) databases.[23,24]

Quantitative real-time RT-qPCR

DNase I-treated RNA (200 ng) was used for reverse transcription (RT) with random hexamers using the Multiscribe RT system (ThermoFisher Scientific) at 48°C for 40 min in a final volume of 50 µl. *DNase I*-treated total RNA was obtained from a pool of commercially available fresh frozen tissue biopsies of five controls subjects (single vial purchased from AMSBIO, Abingdon, Oxford, UK; reference code: R1234106-P, lot number B209050, human normal adult esophageal total RNA); the other RNAs were obtained from fresh frozen tissue biopsies as described above.

RT-qPCR was performed with SYBRGreen, 0.5 μM primers, in an ABI 7500 Real-Time PCR System (ThermoFisher Scientific). All target genes were normalized with the endogenous control (beta-actin) using the ΔΔCt comparative method. Primers are available from the Authors on request.

Western blotting

Proteins were extracted from fresh frozen tissue biopsies of esophagus of achalasia patients and controls by sonication using the Diagenode Bioruptor Pico sonicator System (V 1.1) (10 cycles of 30 on/30 off; 20-60 kHz), in a volume of 50 μl of Laemli buffer 1X. A pool of normal esophageal tissues was commercially available (Abcam, Cambridge, UK, reference code ab30243 - Human esophagus normal tissue lysate - total protein), the other tissues analyzed with western blotting were obtained from fresh frozen tissue biopsies of single cases and controls as reported in Supplementary Tables 1A and 1B. Proteins were visualized on Coomassie Blue gel for quality and quantity control. Western blot analysis was performed by SDS gel electrophoresis and transfer onto nitrocellulose membrane, using the TransBlot system (Bio-Rad Laboratories, Segrate, Italy). Primary antibodies used were the following: rabbit anti-INPP4B diluted 1:200 (Abcam); rabbit anti-c-KIT (Abcam) diluted 1:200; mouse anti-vinculin (Sigma-Aldrich, St. Louis, MO, USA) diluted at 1:5000; mouse anti-GAPDH 1:10000 (Abcam); anti p-Akt (Ser473), anti p-Akt (Thr308), anti Akt (Cell Signaling, Leiden, Netherlands), anti β-actin 1:10000 (Sigma-Aldrich). HRPO-conjugated secondary antibodies (Sigma-Aldrich) were diluted 1:35000 in blocking solution. Bands were visualized by the ECL method Supernova (Cyanagen, Bologna, Italy) using the Chemidoc XRS+ Imager and densitometric analysis was performed with Image lab Software (Bio-Rad Laboratories). All western blot analyses were

performed at least in duplicate for each protein extract from each patient and control tissue biopsy.

Immunohistochemistry

Immunohistochemistry was performed on paraffin-embedded adult human esophagus tissues according to protocols validated in our laboratory.[25] Immunohistochemistry analyses and image acquisitions were performed in our laboratory at the University of Bologna. Briefly, tissue sections were treated to remove paraffin embedding by sequential washes in xylene and graded ethanol. Antigen unmasking was performed by heating sections at 95°C in 10 mM Sodium citrate buffer, pH 6.0, for 10 min and subsequent cooling at room temperature for 30 min. To reduce endogenous peroxidases, tissue sections were treated with an ad hoc blocking kit (GeneTex Inc., Irvine, CA, USA) and incubated for 16 h at 4°C with the same primary antibodies used for western blotting, but diluted 1:50. 3,3'-diaminobenzidine staining was performed according to standard protocols (DAB500 IHC Select® kit, Merck Millipore, Darmstadt, Germany). Scores were assigned based on the intensity of DAB staining (0 = no staining; + = 10-50% staining; ++ = 50-90% staining; +++ = ≥90% staining of the areas; all images were acquired at 10x magnification) according to standard pathological assessment.[26] Three expert observers independently evaluated the images (E.B., F.B. and R. De G.), and their analyses were blinded regarding control *vs*. achalasia state. Image capturing of achalasia and control tissues was performed on a Nikon microscope using DS-5M digital camera (Nikon Instruments, Düsseldorf, Germany).

Statistical analysis

Quantitative difference in densitometry of western blots was performed with the Student's t-test option of GraphPad Quickstat calculator; statistical differences for the scores assigned to IHC samples from tissue biopsies was performed with Fisher's Test (4 x 2 contingency table) using the program Vassarstats.

Results

Whole transcriptome analysis via RNAseq

Total RNA extracted from esophageal biopsies of four cases (2F; age range: 30-58 yrs) and four controls (3F; age range: 27-50 yrs) was used for library preparation and sequencing on Illumina HiScan SQ platform. Raw data showing the total amount of reads/library and the mean coverage are reported in Supplementary Table 2, along with the mean coverage for each sample. Quantitative data analysis using Bioconductor from R package identified 111 genes with differential expression between cases and controls at a $P \leq 10^{-3}$ (Table 1). Compared to controls, 77 genes were downregulated and 34 genes were upregulated in the achalasia group. Hierarchical clustering considering the 111 genes was performed using MEV v4.8.1. As shown in the heat map in Figure 1A, a concordant signature of up- and down-regulation expression was evident between cases and controls. Analysis using PANTHER Functional classification test (PANTHER GO Slim Process) led us to functionally map a total of 109 out of the 111 differentially expressed genes to different biological processes, including, amongst others, cell adhesion, biogenesis, developmental, immune and metabolic processes and response to stimuli (http://www.pantherdb.org/chart/pantherChart.jsp?listType=1&filterLevel=1&type=2&chartType=1&save=yes&basketItems=all&zoom=1.25&trackingId=4DCA8C9D00F5C4649E3257CE82CFAC3E) (Figure 1B). PANTHER Over-representation Test

analysis was performed against the *H. sapiens* gene database, showing a set of over-represented biological processes in achalasia, including, amongst others, phosphorylation, the MAPK cascade signaling (including intracellular signal transduction and cell communication), regulation of phosphate metabolism and developmental processes, e.g. cell differentiation and death (FDR< 0.05; Table 2).

Network analysis was performed with STRING using the list of genes (the previously identified 111 genes) reported in Table 1, using the *H. sapiens* database as model organism, and the "whole genome" option as statistical background. A number of 104 out of 111 genes matched the STRING protein database and were included in the analysis (https://string-db.org/cgi/network.pl?taskId=u9O5yLo4Lf2G). Several pathways were identified that showed a functional enrichment for biological processes, such as regulation of development, cell differentiation, angiogenesis and vascular architecture, with significant *P* values reported in Table 3. Many protein-protein interactions converged on c-KIT (Figure 1C).

Among the dysregulated genes in achalasia, those differentially expressed with a significant $P \leq 10^{-4}$ were selected for further investigation, including *CYR61*, *CTGF*, c-*KIT*, *EGR1*, *LIF* and *CD69* (downregulated); and *AKAP6*, and *INPP4B* (overexpressed) (Table 1). To validate the data from whole transcriptome analysis, we performed quantitative real-time RT-qPCR using the total RNA of already sequenced samples (including two patients and one control). For each real-time RT-qPCR, raw data were normalized on a commercial pool of human normal esophagus RNA from fresh frozen tissue biopsies of five individuals (AMSBIO), using the ΔΔCt method. Data reported in Figure 1D show independent technical replicates (same case-control samples, independent retro-transcription and real-time processes). A significant dysregulation of expression was confirmed for *c-KIT* and *INPP4B* (Figure 1D). These

findings prompted us to focus on these two molecular targets, i.e. *c-KIT* and *INPP4B*, which were down- and up-regulated, respectively.

Protein analysis of INPP4B and c-KIT confirmed the RNAseq data

The protein expression of c-KIT and INPP4B was studied by western blotting. In these experiments, control samples included a pool of normal esophageal tissues (Abcam) from five subjects in addition to control tissues obtained from single individual control subjects. Western blotting analysis for each tissue lysate was performed at least in two independent experiments, i.e. technical replicates. Equal amount of proteins was loaded for each sample and intensities were normalized using reference proteins. Representative examples of the protein patterns observed for c-KIT, INPP4B and reference proteins were reported in Figure 2A. Densitometric analysis of western blots was performed as indicated in Figure 2B. All cases and controls included in the western blotting analysis were reported in Supplementary Tables 1A and 1B. c-KIT downregulation was confirmed in tissue biopsies of achalasia patients compared to controls (P= 0.0003, Student's t-test; Figure 2B), whereas INPP4B overexpression was significantly detectable in achalasia patients *vs.* controls (P=0.0381; Student's t-test, Figure 2B).

Immunohistochemistry analysis was performed in order to confirm the western blot data and to determine the cellular localization of the proteins herein identified by western blot. The density of c-KIT immunoreactive cells (mainly with the typical shape of ICC) was lower in achalasia than in controls (Fisher's exact test, P= 0.0005, Figure 3A). Compared to controls, INPP4B immunoreactivity was more intense in achalasia patients. In INPP4B-positive cases, the immunoreactive signal was present in different cells including muscle cells and myenteric ganglia. INPP4B expression in

the normal tissues was very low or virtually absent (Fisher's exact test, *P*= 0.0023; Figure 3B).

Phospho-Akt is down regulated in achalasia

As INPP4B is a negative regulator of Akt signaling, we investigated Akt phosphorylation status. Equal amount of proteins was loaded for each sample and intensities were normalized using reference proteins. Representative examples of the phosphorylation patterns observed for the two phosphorylation sites in Akt (Ser473, and Thr308) were reported in Figure 4A. Densitometric analysis, performed according to our previously published data,[27] revealed that tissue samples from achalasia patients presented a reduced Akt phosphorylation, in particular the phosphorylation at Ser473 was significantly decreased compared to control tissues (*P*=0.0495, Student's t-test; Figure 4B).

Discussion

Primary achalasia causes significant impairment of esophageal motility leading to symptom generation and overall reduced patients' quality of life. This esophageal dysmotility of the esophagus has a complex etio-pathogenesis. Recent findings indicate that both an inflammatory / immune-mediated insult, as exhibited by myenteric ganglionitis (likely driven by neurotropic, e.g. herpes, virus infection)[28] and circulating anti-neuronal antibodies, play a pathogenetic role. A genetic predisposition conferred by HLA genetic background[20] can contribute to neural abnormalities underlying achalasia. A predominant genetic component has been identified in well-defined conditions such as 'triple A' (also referred to Allgrove's syndrome), where mutations in the ALADIN gene[14] were found in familial clusters. Other data derive

from *NOS1*, which encodes for the neuronal nitric oxide synthase. A stop codon mutation of this gene has been reported in a family where two children manifested a very severe clinical phenotype dominated by achalasia.[13] Nevertheless, in the majority of cases the factors causing achalasia remain to be elucidated. As a consequence, the available therapeutic approaches are far from targeting the actual mechanisms leading to the neural impairment recognized to be the *primum movens* of this severe esophageal disorder. New understanding of achalasia, involving a deeper knowledge of the attendant molecular mechanisms, should aim to a better patient management and stop the disease at early stages. Therefore, the present study attempted to decipher the altered molecular pathways in patients with achalasia. We strategically used esophageal tissues from achalasic patients and examined gene expression via whole transcriptome analysis in order to provide novel targets for a therapeutic approach. From the RNAseq data we detected 111 genes with an altered expression. Functional classification and over-representation analysis of the biological processes, where these genes mapped, was performed with two different bioinformatic tools, PANTHER and STRING. Results showed a significant over-representation of phosphorylation processes, intracellular signaling, cell communication and development /differentiation processes, including cell death. These data suggest that an imbalance of cell growth/survival *vs.* cell death may cause the defects observed in the achalasia tissues, not only in term of neuron loss, but also as an overall tissue degeneration. Notably, in a recent study, Palmieri et al. performed transcriptome analysis on tissues of primary achalasia patients and identified a significant enrichment of neuro-muscular and neuro-immune processes. These data support the concept that achalasia results from degenerative alterations / loss of myenteric

neurons mainly evoked by a chronic inflammatory infiltrate targeting the myenteric plexus.[29]

Among the genes with significant dysregulation, we confirmed by real-time qPCR *c-KIT* downregulation and *INPP4B* upregulation, respectively. *c-KIT* significant downregulation, validated both via western blot and immunohistochemistry, confirms and expands previously reported data showing a loss of ICC network in tissues of patients with primary achalasia.[9] Our data highlighting a significant decrease of c-KIT expression in human achalasia support the concept that stem cell factor, the major ligand to c-KIT, cannot mediate ICC maintenance and survival. Although we did not look into specific apoptotic mechanisms, it is likely that a programmed cell death can involve ICC in achalasia.[30] Since ICC play a role in esophageal motility, their depletion can contribute to the deranged mechanisms leading to altered motility in achalasia.[31]

The second gene for which we were able to confirm an altered expression at the protein level is INPP4B, encoding for inositol polyphosphate-4-phosphatase type II B, a negative regulator of Akt.[32,33] The expression of this phosphatase was upregulated in many cell types in tissues from achalasic patients, indicating a general increase in inhibitory signals for cell survival, a mechanism stimulated by Akt-dependent pathways.[32] Thus, an INPP4B increased expression can be correlated to the enrichment in genes involved in cell death. Notably, in achalasia tissues we observed a decrease in the phosphorylation of the Ser473 in Akt, which is a key phosphorylation step for its activation and function. Therefore, it may be postulated that in achalasia the altered molecular signaling led to an overall impaired cell survival, which, in the long term, generates a permanent tissue damage. Thus, one can assume that also ICCs, in addition to neurons, can be affected. Since many studies

have investigated the Akt / INPP4B pathway as a potential "druggable" route to block tumor proliferation,[33,34] the development of *ad hoc* molecules may become relevant for patients with primary achalasia.

In conclusion, our study highlights the altered expression of two distinct genes, i.e. c-KIT and INPP4B down- and up-regulation, in patients with primary achalasia. Our results may provide a basis for future research aimed at investigating novel therapeutic targets for patients with primary achalasia.

Acknowledgements

The authors wish to thank all patients that participated in the study. We thank Drs. A. Gori, and V. Bertakis and Ms. G. Galiazzo for technical help.

References

1. Boeckxstaens GE, Zaninotto G, Richter JE. Achalasia. Lancet 2014;383:83-93.

2. Moonen A, Boeckxstaens G. Current diagnosis and management of achalasia. J Clin Gastroenterology 2014;48:484-90.

3. Kahrilas PJ, Boeckxstaens G. The spectrum of achalasia: lessons from studies of pathophysiology and high resolution manometry. Gastroenterology 2013;145:954-65.

4. Di Nardo G, Tullio-Pelet A, Annese V, et al. Idiopathic achalasia is not allelic to alacrima achalasia adrenal insufficiency syndrome at the ALADIN locus. Dig Liver Dis 2005;37:312-5.

5. Goldblum, JR, Rice, TW, Richter JE. Histopathologic features in esophagomyotomy specimens from patients with achalasia. Gastroenterology 1996;111:648-54.

6. Roman S, Gyawali CP, Xiao Y, Pandolfino JE, Kahrilas PJ. The Chicago classification of motility disorders: an update. Gastrointest Endosc Clin North Am 2014;24:545-61.

7. Boeckxstaens GE, Annese V, des Varannes SB, et al. European Achalasia Trial Investigators. Pneumatic dilation versus laparoscopic Heller's myotomy for idiopathic achalasia. N Engl J Med 2011;364:1807-16.

8. Ates F, Vaezi MF. The Pathogenesis and management of achalasia: Current status and future directions. Gut Liver 2015;9:449-63.

9. Gockel I, Bohl JR, Eckardt VF, Junginger T. Reduction of interstitial cells of Cajal (ICC) associated with neuronal nitric oxide synthase (n-NOS) in patients with achalasia. Am J Gastroenterol 2008;103:856-64.

10. Saraiva MJM, Birken S, Costa PP, Goodman DS. Amyloid fibril protein in familial amyloidotic polyneuropathy, Portuguese type: definition of molecular abnormality in transthyretin (prealbumin). J Clin Invest 1984;74:104-19.

11. Sodikoff JB, Lo AA, Shetuni BB, Kahrilas PJ, Yang GY, Pandolfino JE. Histopathologic patterns among achalasia subtypes. Neurogastroenterol Motil 2016;28:139-45.

12. Storch WB, Eckardt VF, Junginger T. Complement components and terminal complement complex in oesophageal smooth muscle of patients with achalasia. Cell Mol Biol (Noisy-le-grand) 2002;48:247-52.

13. Shteyer E, Edvardson S, Wynia-Smith SL, et al. Truncating mutation in the nitric oxide synthase 1 gene is associated with infantile achalasia. Gastroenterology

2015;148:533-36.

14. Tullio-Pelet A, Salomon R, Hadj-Rabia S, et al. Mutant WD-repeat protein in triple-A syndrome. Nat Genet 2000;26:332-5.

15. Becker J, Haas SL, Mokrowiecka A, et al. The HLA-DQβ1 insertion is a strong achalasia risk factor and displays a geospatial north-south gradient among Europeans. Eur J Hum Genet 2016;24:1228-31.

16. Verne GN, Sallustio JE, Eaker EY. Anti-myenteric neuronal antibodies in patients with achalasia. A prospective study. Dig Dis Sci 1997;42:307-13.

17. Ruiz-de-León A, Mendoza J, Sevilla-Mantilla C, et al. Myenteric antiplexus antibodies and class II HLA in achalasia. Dig Dis Sci 2002;47:15-19.

18. Latiano A, De Giorgio R, Volta U, et al. HLA and enteric antineuronal antibodies in patients with achalasia. Neurogastroenterol Motil 2006;18:520-25.

19. De la Concha EG, Fernandez-Arquero M, Mendoza JL, et al. Contribution of HLA class II genes to susceptibility in achalasia. Tissue Antigens 1998;52:381-84.

20. Gockel I, Becker J, Wouters MM, et al. Common variants in the HLA-DQ region confer susceptibility to idiopathic achalasia. Nat Genet 2014;46:901-4.

21. Nannini M, Astolfi A, Urbini M, et al. Integrated genomic study of quadruple-WT GIST (KIT/PDGFRA/SDH/RAS pathway wild-type GIST). BMC Cancer. 2014;14:685.

22. Huang X, Muruganujan A, Tang H, et al. PANTHER version 11: expanded annotation data from Gene Ontology and Reactome pathways, and data analysis tool enhancements. Nucleic Acids Research, 2017;45:D183–9.

23. Szklarczyk D, Morris JH, Cook H, et al. The STRING database in 2017: quality-controlled protein-protein association networks, made broadly accessible. Nucleic Acids Res. 2017; 45: D362–D368.

24. Szklarczyk D, Franceschini A, Wyder S, et al. STRING v10: protein-protein interaction networks, integrated over the tree of life. Nucleic Acids Res. 2015 Jan; 43:D447-52.

25. Bonora E, Bianco F, Cordeddu L, et al. Mutations in RAD21 disrupt regulation of APOB in patients with chronic intestinal pseudo-obstruction. Gastroenterology 2015;148:771-82.e11.

26. Couch G, Redman JE, Wernisch L, Newton R, et al. The Discovery and Validation of Biomarkers for the Diagnosis of Esophageal Squamous Dysplasia and Squamous. Cancer Prev Res (Phila). 2016;9:558-66.

27. Buontempo F, Orsini E, Lonetti A, et al. Synergistic cytotoxic effects of bortezomib and CK2 inhibitor CX-4945 in acute lymphoblastic leukemia: turning off the prosurvival ER chaperone BIP/Grp78 and turning on the pro-apoptotic NF-κB. Oncotarget. 2016;7:1323-40.

28. Moonen A, Boeckxstaens GE. Finding the right treatment for achalasia treatment: Risks, efficacy, complications. Curr Treat Options Gastroenterol 2016;14:420-28.

29. Palmieri O, Mazza T, Merla A, et al. Gene expression of muscular and neuronal pathways is cooperatively dysregulated in patients with idiopathic achalasia. Sci Rep 2016;6:31549.

30. Gibbons SJ, De Giorgio R, Faussone Pellegrini MS, et al. Apoptotic cell death of human interstitial cells of Cajal. Neurogastroenterol Motil 2009;21:85-93.

31. Farrugia G. Histologic changes in diabetic gastroparesis. Gastroenterol Clin North Am. 2015;44:31-8.

32. Rodgers SJ, Ferguson DT, Mitchell CA, Ooms LM. Regulation of PI3K effector signalling in cancer by the phosphoinositide phosphatases. Biosci Rep 2017;10:37(1).

33. Chew CL, Chen M, Pandolfi PP. Endosome and INPP4B. Oncotarget 2016;7:5-6.

34. Li Chew C, Lunardi A, Gulluni F, et al. In vivo role of INPP4B in tumor and metastasis suppression through regulation of PI3K-AKT signaling at endosomes. Cancer Discov 2015;5:740-51.

Table 1. Genes differentially expressed in achalasia.

Genes overexpressed in achalasia are labeled in red. Green shadowed area indicates the genes with a $P \leq 10^{-4}$.

ENSEMBL transcript ID	GENE name	log2 Fold Change	*P* value
ENST00000451137	*CYR61*	*-2.99*	*9.71E-06*
ENST00000367976	*CTGF*	*-2.74*	*1.19E-05*
ENST00000513000	*INPP4B*	*1.63*	*1.42E-04*
ENST00000288135	*KIT*	*-1.48*	*4.17E-04*
ENST00000249075	*LIF*	*-2.40*	*4.23E-04*
ENST00000239938	*EGR1*	*-1.95*	*4.65E-04*
ENST00000228434	*CD69*	*-3.84*	*4.94E-04*
ENST00000280979	*AKAP6*	*1.63*	*7.28E-04*
ENST00000296464	*HSPA4L*	*1.07*	*8.99E-04*
ENST00000319653	FMN2	2.03	1.11E-03
ENST00000517956	FBXO32	1.26	1.12E-03
ENST00000265634	NPTX2	-1.88	1.20E-03
ENST00000550683	ACVRL1	-1.14	1.25E-03
ENST00000378827	BMP2	-1.99	1.51E-03
ENST00000371852	CH25H	-3.06	1.56E-03
ENST00000284669	KLHL41	2.43	1.58E-03
ENST00000436924	BRE	2.70	1.60E-03
ENST00000561981	FRRS1L	1.51	1.62E-03
ENST00000307792	SEMA3E	1.07	1.66E-03
ENST00000330871	SOCS3	-2.47	2.07E-03
ENST00000331569	ZNF703	1.18	2.30E-03
ENST00000305988	ADRB2	-1.41	2.47E-03
ENST00000420022	ADM5	-1.80	2.58E-03
ENST00000297316	SOX17	-1.82	2.76E-03
ENST00000252590	PLVAP	-1.29	2.77E-03
ENST00000256103	PMP2	-2.28	2.87E-03
ENST00000329099	FAM101B	-1.32	3.11E-03
ENST00000287814	TIMP4	-1.25	3.12E-03
ENST00000300177	GREM1	-2.58	3.29E-03
ENST00000485685	GGNBP2	-1.78	3.40E-03
ENST00000365328	RN7SK	-1.61	3.41E-03
ENST00000284878	CXADR	2.20	3.47E-03
ENST00000296046	CPA3	-1.76	3.52E-03
ENST00000302754	JUNB	-1.73	3.74E-03
ENST00000437551	PAX8-AS1	1.36	3.74E-03
ENST00000322507	COL12A1	-1.10	3.80E-03
ENST00000307637	C3AR1	-1.86	3.82E-03
ENST00000340695	SCXA	2.40	3.88E-03
ENST00000322954	UACA	0.94	3.89E-03

ENST00000055682	KIAA2022	1.00	3.92E-03
ENST00000379374	PHEX	-3.10	3.98E-03
ENST00000357949	SERTAD1	-1.45	4.02E-03
ENST00000230990	HBEGF	-2.36	4.08E-03
ENST00000359534	KCNK5	-2.25	4.16E-03
ENST00000224605	GDF10	-1.64	4.17E-03
ENST00000396184	PDE1C	1.02	4.32E-03
ENST00000373509	PIM1	-2.29	4.33E-03
ENST00000408965	CEBPD	-1.45	4.59E-03
ENST00000267984	MESDC1	-1.17	4.82E-03
ENST00000329608	CSF1	-1.16	4.92E-03
ENST00000344120	SPRY4	-1.18	5.13E-03
ENST00000395076	PPM1A	0.85	5.16E-03
ENST00000350896	MSR1	-1.37	5.21E-03
ENST00000366667	AGT	-1.68	5.22E-03
ENST00000263370	ITPKC	-1.75	5.24E-03
ENST00000259989	FGFBP2	-1.75	5.24E-03
ENST00000311922	TRIB1	-2.74	5.24E-03
ENST00000608521	MIR663A	2.80	5.25E-03
ENST00000377103	THBD	-2.31	5.27E-03
ENST00000422542	AC005682,5	-1.34	5.32E-03
ENST00000396037	ST8SIA1	1.75	5.39E-03
ENST00000264805	PDE5A	2.61	5.58E-03
ENST00000400546	NCAM2	-1.27	5.65E-03
ENST00000369026	MCL1	-1.16	6.00E-03
ENST00000515896	RNA5-8SP6	1.12	6.20E-03
ENST00000399799	ROCK1	0.96	6.23E-03
ENST00000273153	CSRNP1	-1.74	6.25E-03
ENST00000244221	PAIP2B	1.09	6.25E-03
ENST00000376414	GPR183	-1.77	6.40E-03
ENST00000500741	DYNLL1-AS1	1.16	6.57E-03
ENST00000308086	THAP2	0.91	6.67E-03
ENST00000274063	SFRP2	-1.92	6.68E-03
ENST00000290551	BTG2	-1.53	6.72E-03
ENST00000380392	C2CD4B	-2.57	6.78E-03
ENST00000410087	CERKL	-1.36	6.83E-03
ENST00000367558	RGS16	-2.28	7.09E-03
ENST00000256257	RNF122	-1.65	7.10E-03
ENST00000367511	FAM129A	0.64	7.12E-03
ENST00000592790	VMP1	-2.93	7.17E-03
ENST00000323040	GPR4	-1.97	7.27E-03
ENST00000307851	HAVCR2	-1.68	7.40E-03
ENST00000324559	ANO5	0.96	7.62E-03
ENST00000328041	SLC24A3	-1.35	7.63E-03
ENST00000311734	IL1RL1	-3.50	7.72E-03
ENST00000373313	MAFB	-1.65	8.05E-03

ENST00000382723	MSX1	-2.11	8.32E-03
ENST00000379731	B4GALT1	-1.49	8.33E-03
ENST00000329399	PDLIM1	-1.46	8.42E-03
ENST00000369583	DUSP5	-1.58	8.43E-03
ENST00000332029	SOCS1	-1.69	8.47E-03
ENST00000441535	FMO2	-1.27	8.55E-03
ENST00000256951	EMP1	-2.33	8.71E-03
ENST00000239223	DUSP1	-1.08	8.75E-03
ENST00000330106	CEND1	-2.85	8.84E-03
ENST00000498165	PPM1L	1.08	8.87E-03
ENST00000506002	MTND6P4	1.03	8.91E-03
ENST00000244050	SNAI1	-1.59	8.93E-03
ENST00000380874	FOXC1	-1.77	8.94E-03
ENST00000396073	ENAM	2.83	9.03E-03
ENST00000272928	ACKR3	-1.31	9.04E-03
ENST00000379359	RGCC	-1.11	9.22E-03
ENST00000333926	CISD1	0.80	9.30E-03
ENST00000367996	ADAMTS4	-4.18	9.37E-03
ENST00000380079	STEAP4	-2.07	9.38E-03
ENST00000413366	PRKCA	1.03	9.39E-03
ENST00000215794	USP18	-1.45	9.57E-03
ENST00000305352	S1PR1	-1.27	9.74E-03
ENST00000306065	ANKRD27	0.67	9.81E-03
ENST00000222390	HGF	-2.02	9.83E-03
ENST00000358432	EPHA2	-1.13	9.85E-03
ENST00000270001	ZFP14	0.88	9.89E-03

535

536

Table 2. Output of PANTHER Over-representation test of biological processes enriched for the genes differentially expressed in achalasia tissues, compared to H. sapiens gene PANTHER database.

PANTHER GO Slim Biological process	*H. sapiens*	Achalasia	Expected	Fold enrichment	Hierarchy (+/-)	raw *P* value	False Discovery Rate
Protein phosphorylation	81	4	.42	9.53	+	9.80e-04	3.99e-02
MAPK cascade	340	9	1.76	5.11	+	8.19e-05	6.66e-03
• intracellular signal transduction	1071	17	5.55	3.06	+	4.05e-05	4.94e-03
• signal transduction	2318	24	12.01	2.00	+	1.01e-03	3.54e-02
• Cell communication	2686	26	13.91	1.87	+	1.39e-03	3.76e-02
Regulation of catalytic activity	359	9	1.86	4.84	+	1.22e-04	7.47e-03
• regulation of molecular function	441	9	2.28	3.94	+	5.38e-04	2.62e-02
Regulation of phosphate metabolic process	537	12	2.78	4.31	+	2.64e-05	6.44e-03
Developmental process	1501	18	7.78	2.32	+	1.03e-03	3.13e-02

Only results with False Discovery Rate<0.05 are reported in the table.

Table 3: Output of STRING (protein-protein interaction and biological processes) for genes differentially regulated from whole transcriptome analysis of achalasia tissues.

	Pathway ID and description	Count in gene set	False Discovery Rate *P* values
Biological Process (GO)	GO 0051094 positive regulation of developmental process	29	1.97e-10
	GO 1901342 regulation of vascular development	15	8.62e-10
	GO 0045597 positive regulation of cell differentiation	24	1.44e-09
	GO 004565 regulation of angiogenesis	14	2.7e-09
	GO 2000026 regulation of multicellular organismal development	31	3.31e-09
Molecular function (GO)	GO 0001228 transcriptional activator activity, RNA polymerase II transcription regulatory region sequence-specific binding	9	0.0483
	GO 0005515 protein binding	40	0.0483
	GO 0008083 growth factor activity	3	0.0483
Cellular component (GO)	GO 005615 extracellular space	20	0.00342
	GO 0009986 cell surface	14	0.00552

Statistical background selected for the enrichment analysis set to "whole genome".

Figure Legends

Figure 1. Differentially expressed genes in achalasia tissue. (A) Heat map showing the concordant differential expression observed in the tissues from achalasia patients compared to controls (for the genes reported in Table 1). Elaborated with MeV v4.8.1. (B) Biological processes of genes (GO-Slim Biological processes) differentially expressed in achalasia, as identified by PANTHER Functional Classification analysis. (C) Graphical output of significantly enriched protein-protein interactions determined with STRING analysis, showing the results of the 104 out of 111 dysregulated genes in achalasia, compared with data present in the STRING databases. The different colors in the figure inset identify the evidence for the different interactions (known; predicted; identified with other means, such as co-expression, data mining, and protein homology). The red square indicates c-KIT. (D) Real-time qRT-PCR data for *c-KIT* and *INPP4B*. Data from case and control tissue biopsies were normalized on a commercial pool of control tissue biopsies from esophagus. Student's t-test was performed and *P* values are indicated. Bars indicate standard deviations.

Figure 2. Western blot analysis of differentially expressed genes. (A) Example of the protein expression profiles in achalasia tissues compared to control samples for c-KIT and INPP4B. Western blotting was repeated in at least two independent experiments. (B) Densitometric analysis of the relative intensities for c-KIT and INPP4B. Quantitative data (mean values ± standard deviation) from different experiments obtained from each individual were compared using Student's t-test for statistical analysis. For each sample, densitometric values were normalized on reference protein (vinculin). All experiments were carried out at least twice. Bars indicated standard deviations. *P* values are indicated in the graphs.

Figure 3. Immunostaining for c-KIT (A) and INPP4B (B). (A) Examples of the expression pattern for c-KIT in tissue biopsies from control (left) and achalasia patients (right). Arrows indicate the positive staining for c-KIT. c-KIT staining color histograms of controls (n=6) and cases (n=18) represent the number of samples assessed according to the semi-quantitative score. c-KIT immunolabeling differences in cases *vs.* controls were assessed by Fisher's exact test. (B) Examples of the expression pattern for INPP4B in tissue biopsies from control (left) and achalasia patients (right). INPP4B staining color histograms of controls (n=6) and cases (n=22) represent the number of samples assessed according to the semi-quantitative score. INPP4B immunolabeling differences in cases *vs*. controls were assessed by Fisher's exact test. Scale bars are 100µm as indicated.

Figure 4. Phospho-Akt is down regulated in achalasia. (A) Example of the protein expression profiles in achalasia tissues compared to control samples of phospho-Akt (Ser473; Thr308) and total Akt. (B) Quantitative data (mean values ± standard deviation) from different experiments (performed in duplicate) obtained from each individual were compared using Student's t-test. For each sample, densitometric values were normalized on reference protein (β-actin). The significantly different relative phospho-Akt (Ser473) levels comparing achalasia *vs*. control tissues, were reported in the histogram (P=0.0495, Student's t-test). Bars indicate standard deviations.

Supplementary Table 1: **Clinical and epidemiological data of achalasia patients (a) and controls (b)**

a) Achalasia

ACHA pts ID	Sex	Age	Age at diagnosis	LES basal pressure (mm Hg)	Duration of symptoms before diagnosis(yrs)	Type of molecular analysis
ITA_ACHA77	M	43	30	15	15	wb
ITA_ACHA69	M	84	83	53	20	wb
ITA_ACHA74	M	42	41	22.5	5	wb
ITA_ACHA59	F	51	50	20	3	wb/IHC
ITA_ACHA81	F	24	20	18	5	wb
ITA_ACHA40	F	42	39	28	8	wb
ITA_ACHA17	F	46	45	20	10	wb
ITA_ACHA76	M	55	54	24	10	wb
ITA_ACHA71	F	72	70	15	8	wb
ITA_ACHA34	M	68	67	44	8	RNAseq
ITA_ACHA16	F	25	24	18	2	RNAseq
ITA_ACHA75	F	75	58	15	25	IHC
ITA_ACHA37	F	64	61	18	4	RNAseq/RT-qPCR/wb/IHC
ITA_ACHA34	M	58	57	35	20	/wb
ITA_ACHA02	F	37	34	25	4	wb/IHC
ITA_ACHA73	M	81	78	28	4	wb
ITA_ACHA33	M	68	67	44	2	RNAseq/RT-qPCR/wb/IHC
ITA_ACHA25	M	66	64	22	3	wb
ITA_ACHA78	F	36	36	15	1	IHC
ITA_ACHA66	F	41	40	23	20	wb
BE_ACHA5051	F	16	16	37	6	IHC
BE_ACHA5208	M	69	69	na[a)]	7	IHC
BE_ACHA5691	F	82	82	na	2.5	IHC
BE_ACHA6936	F	20	20	38	2	IHC
BE_ACHA7521	F	63	63	35.3	0.42	IHC
BE_ACHA5466	M	22	22	27.5	1	IHC
BE_ACHA5768	M	44	44	33	1.5	IHC
BE_ACHA6790	F	69	69	35.6	2	IHC
BE_ACHA810	M	61	61	30	15	IHC
BE_ACHA8705	M	65	65	na	10	IHC
BE_ACHA1059	M	28	28	na[a)]	7	IHC
BE_ACHA8154	F	42	42	68	0.58	IHC
BE_ACHA302	M	50	50	51	3	IHC
BE_ACHA479	M	50	50	34	3	IHC
BE_ACHA7818	F	33	33	38	0.17	IHC
BE_ACHA8199	M	24	24	103	6	IHC
BE_ACHA8347	F	21	21	na[b)]	4	IHC

BE_ACHA5260	F	32	32	48.3	2	IHC
BE_ACHA5295	F	35	35	na	6	IHC
BE_ACHA1730	M	57	57	nm	5	IHC
BE_ACHA3017	M	49	49	42.3	2	IHC
BE_ACHA3354	F	49	49	80.3	8	IHC

Legends: na= not available; nm= not measurable; [a)] type I; [b)] type II; wb= western blotting; IHC= immunohistochemistry.

b) controls

ID patients	Age	Sex	Pathology	Surgery	Histology	Type of molecular analysis
ITA_CNT_01	64	F	Gastroesophageal reflux	Antireflux Nissen fundoplication	-	IHC
ITA_CNT_02	45	M	Gastroesophageal reflux	Antireflux Nissen fundoplication	-	IHC
ITA_CNT_03	77	M	Esophageal adenocarcinoma - Siewert II	Total gastrectomy and resection of the distal esophagus (10 cm section above the diaphragmatic hiatus)	Intestinal adenocarcinoma (T3-N1-M0). Tumor-free margins	wb/IHC
ITA_CNT_70	55	M	Megaesophagus	Partial esophagectomy with gastro-esophageal reconstruction		IHC
ITA_CNT_72	87	M	Esophageal adenocarcinoma - Siewert I	Partial esophagectomy with gastro-esophageal reconstruction	Intestinal adenocarcinoma (T2-N1-M0). Tumor-free margins	IHC
ITA_CNT_04	69	M	Esophageal adenocarcinoma - Siewert II	Total gastrectomy and resection of the distal esophagus (10 cm section above the diaphragmatic hiatus)	Intestinal adenocarcinoma (T4-N3-M0). Tumor-free margins	IHC
ITA_CNT_26	49	F	Gastroesophageal reflux	Antireflux Nissen fundoplication	-	RNAseq/wb
ITA_CNT_23	46	F	Gastroesophageal reflux	Antireflux Nissen fundoplication	-	RNAseq/wb/IHC
ITA_CNT_41	66	M	Esophageal adenocarcinoma - Siewert I	Partial esophagectomy with gastro-esophageal reconstruction	Intestinal adenocarcinoma (T2-N1-M0). Tumor-free margins	RNAseq/wb
ITA_CNT_52	57	M	Esophageal adenocarcinoma - Siewert I	Partial esophagectomy with gastro-esophageal reconstruction	Intestinal adenocarcinoma (T3-N3-M0). Tumor-free margins	RNAseq/RT-qPCR/wb/IHC

Supplementary Table S2. Total read number and mean coverage of RNAseq libraries.

Sample ID	Total read number	Mean coverage (X)
ITA_ACHA16	96,763,286	63
ITA_ACHA34	79,986,036	43
ITA_ACHA37	85,671,948	47
ITA_ACHA33	74,486,236	55
ITA_CNT29	70,830,832	36
ITA_CNT26	70,217,988	55
ITA_CNT41	83,327,050	64
ITA_CNT52	81,841,600	68

Supplementary Table 1: **Clinical and epidemiological data of achalasia patients (a) and controls (b)**

a) Achalasia

ACHA pts ID	Sex	Age	Age at diagnosis	LES basal pressure (mm Hg)	Duration of symptoms before diagnosis(yrs)	Type of molecular analysis
ITA_ACHA77	M	43	30	15	15	wb
ITA_ACHA69	M	84	83	53	20	wb
ITA_ACHA74	M	42	41	22.5	5	wb
ITA_ACHA59	F	51	50	20	3	wb/IHC
ITA_ACHA81	F	24	20	18	5	wb
ITA_ACHA40	F	42	39	28	8	wb
ITA_ACHA17	F	46	45	20	10	wb
ITA_ACHA76	M	55	54	24	10	wb
ITA_ACHA71	F	72	70	15	8	wb
ITA_ACHA34	M	68	67	44	8	RNAseq
ITA_ACHA16	F	25	24	18	2	RNAseq
ITA_ACHA75	F	75	58	15	25	IHC
ITA_ACHA37	F	64	61	18	4	RNAseq/RT-qPCR/wb/IHC
ITA_ACHA34	M	58	57	35	20	/wb
ITA_ACHA02	F	37	34	25	4	wb/IHC
ITA_ACHA73	M	81	78	28	4	wb
ITA_ACHA33	M	68	67	44	2	RNAseq/RT-qPCR/wb/IHC
ITA_ACHA25	M	66	64	22	3	wb
ITA_ACHA78	F	36	36	15	1	IHC
ITA_ACHA66	F	41	40	23	20	wb
BE_ACHA5051	F	16	16	37	6	IHC
BE_ACHA5208	M	69	69	na[a)]	7	IHC
BE_ACHA5691	F	82	82	na	2.5	IHC
BE_ACHA6936	F	20	20	38	2	IHC
BE_ACHA7521	F	63	63	35.3	0.42	IHC
BE_ACHA5466	M	22	22	27.5	1	IHC
BE_ACHA5768	M	44	44	33	1.5	IHC
BE_ACHA6790	F	69	69	35.6	2	IHC
BE_ACHA810	M	61	61	30	15	IHC
BE_ACHA8705	M	65	65	na	10	IHC
BE_ACHA1059	M	28	28	na[a)]	7	IHC
BE_ACHA8154	F	42	42	68	0.58	IHC
BE_ACHA302	M	50	50	51	3	IHC
BE_ACHA479	M	50	50	34	3	IHC
BE_ACHA7818	F	33	33	38	0.17	IHC
BE_ACHA8199	M	24	24	103	6	IHC
BE_ACHA8347	F	21	21	na[b)]	4	IHC

BE_ACHA5260	F	32	32	48.3	2	IHC
BE_ACHA5295	F	35	35	na	6	IHC
BE_ACHA1730	M	57	57	nm	5	IHC
BE_ACHA3017	M	49	49	42.3	2	IHC
BE_ACHA3354	F	49	49	80.3	8	IHC

Legends: na= not available; nm= not measurable; [a)] type I; [b)] type II; wb= western blotting; IHC= immunohistochemistry.

b) controls

ID patients	Age	Sex	Pathology	Surgery	Histology	Type of molecular analysis
ITA_CNT_01	64	F	Gastroesophageal reflux	Antireflux Nissen fundoplication	-	IHC
ITA_CNT_02	45	M	Gastroesophageal reflux	Antireflux Nissen fundoplication	-	IHC
ITA_CNT_03	77	M	Esophageal adenocarcinoma - Siewert II	Total gastrectomy and resection of the distal esophagus (10 cm section above the diaphragmatic hiatus)	Intestinal adenocarcinoma (T3-N1-M0). Tumor-free margins	wb/IHC
ITA_CNT_70	55	M	Megaesophagus	Partial esophagectomy with gastro-esophageal reconstruction		IHC
ITA_CNT_72	87	M	Esophageal adenocarcinoma - Siewert I	Partial esophagectomy with gastro-esophageal reconstruction	Intestinal adenocarcinoma (T2-N1-M0). Tumor-free margins	IHC
ITA_CNT_04	69	M	Esophageal adenocarcinoma - Siewert II	Total gastrectomy and resection of the distal esophagus (10 cm section above the diaphragmatic hiatus)	Intestinal adenocarcinoma (T4-N3-M0). Tumor-free margins	IHC
ITA_CNT_26	49	F	Gastroesophageal reflux	Antireflux Nissen fundoplication	-	RNAseq/wb
ITA_CNT_23	46	F	Gastroesophageal reflux	Antireflux Nissen fundoplication	-	RNAseq/wb/IHC
ITA_CNT_41	66	M	Esophageal adenocarcinoma - Siewert I	Partial esophagectomy with gastro-esophageal reconstruction	Intestinal adenocarcinoma (T2-N1-M0). Tumor-free margins	RNAseq/wb
ITA_CNT_52	57	M	Esophageal adenocarcinoma - Siewert I	Partial esophagectomy with gastro-esophageal reconstruction	Intestinal adenocarcinoma (T3-N3-M0). Tumor-free margins	RNAseq/RT-qPCR/wb/IHC

Supplementary Table S2. Total read number and mean coverage of RNAseq libraries.

Sample ID	Total read number	Mean coverage (X)
ITA_ACHA16	96,763,286	63
ITA_ACHA34	79,986,036	43
ITA_ACHA37	85,671,948	47
ITA_ACHA33	74,486,236	55
ITA_CNT29	70,830,832	36
ITA_CNT26	70,217,988	55
ITA_CNT41	83,327,050	64
ITA_CNT52	81,841,600	68

Supporting Material for reviewers Only

New! **PANTHER13.1 released.**

Analysis Summary: Please report in publication

Analysis Type: PANTHER Overrepresentation Test (Released 20171205)

Annotation Version and Release Date: PANTHER version 13.1 Released 2018-02-03

Analyzed List: Client Text Box Input (Homo sapiens) Change

Reference List: Homo sapiens (all genes in database) Change

Annotation Data Set: PANTHER GO-Slim Biological Process

Test Type: Fisher's Exact with FDR multiple test correction Binomial

Results

	Reference list	Client Text Box Input
Mapped IDs:	21042 out of 21042	105 out of 109
Unmapped IDs:	0	7
Multiple mapping information:	0	4

Export results View: -- Please select a chart to display --

Displaying only results with False Discovery Rate < 0.05; click here to display all results

	Homo sapiens (REF)	Client Text Box Input (Hierarchy NEW!)					
PANTHER GO-Slim Biological Process	#	#	expected	Fold Enrichment	+/-	raw P value	FDR
protein phosphorylation	81	4	.42	9.53	+	9.80E-04	3.99E-02
MAPK cascade	340	9	1.76	5.11	+	8.19E-05	6.66E-03
↳intracellular signal transduction	1071	17	5.55	3.06	+	4.05E-05	4.94E-03
↳signal transduction	2318	24	12.01	2.00	+	1.01E-03	3.54E-02
↳cell communication	2686	26	13.91	1.87	+	1.39E-03	3.76E-02
regulation of catalytic activity	359	9	1.86	4.84	+	1.22E-04	7.47E-03
↳regulation of molecular function	441	9	2.28	3.94	+	5.38E-04	2.62E-02
regulation of phosphate metabolic process	537	12	2.78	4.31	+	2.64E-05	6.44E-03
developmental process	1501	18	7.78	2.32	+	1.03E-03	3.13E-02

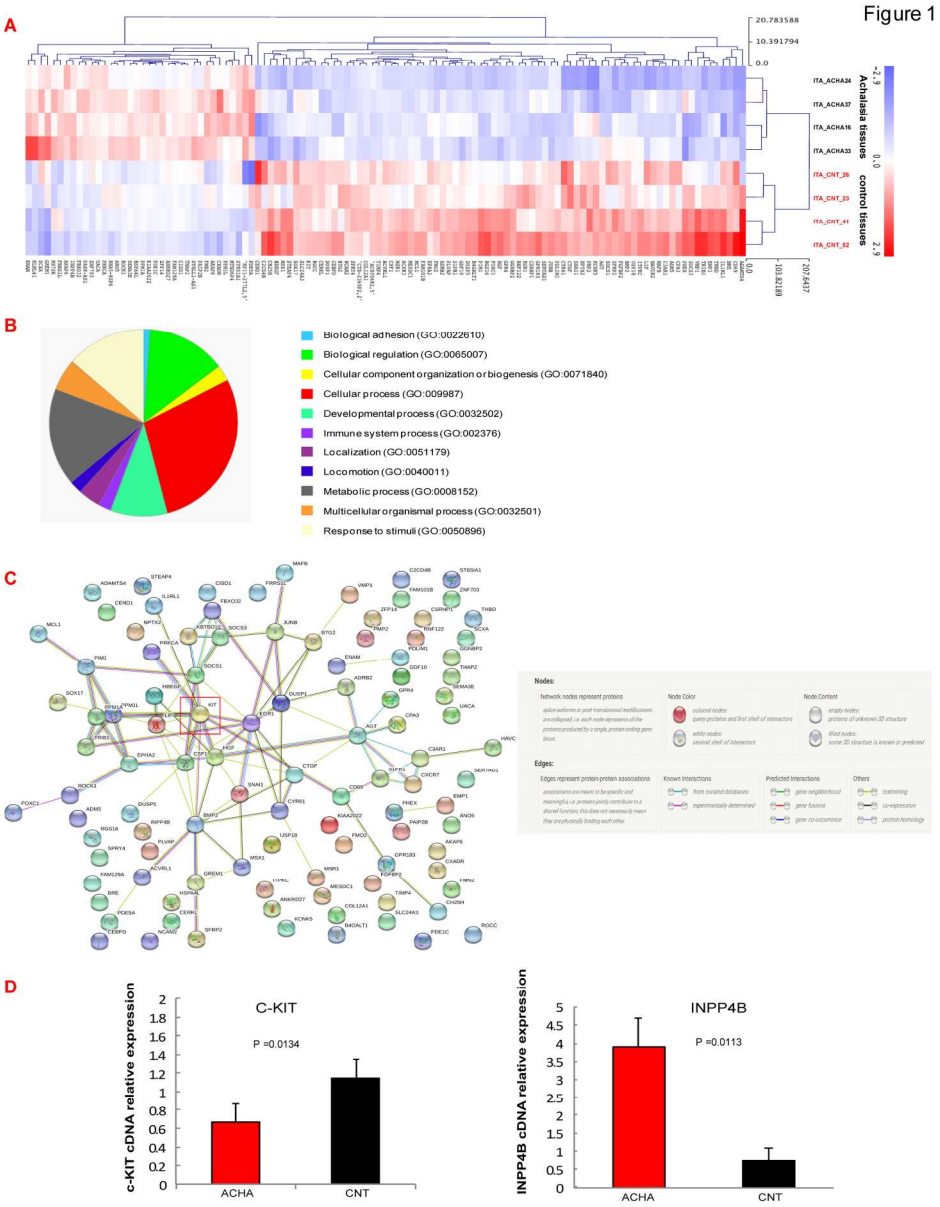

Figure 1. Differentially expressed genes in achalasia tissue. (A) Heat map showing the concordant differential expression observed in the tissues from achalasia patients compared to controls (for the genes reported in Table 1). Elaborated with MeV v4.8.1. (B) Biological processes of genes (GO-Slim Biological processes) differentially expressed in achalasia, as identified by PANTHER Functional Classification analysis. (C) Graphical output of significantly enriched protein-protein interactions determined with STRING analysis, showing the results of the 104 out of 111 dysregulated genes in achalasia, compared with data present in the STRING databases. The different colors in the figure inset identify the evidence for the different interactions (known; predicted; identified with other means, such as co-expression, data mining, and protein homology). The red square indicates c-KIT. (D) Real-time qRT-PCR data for c-KIT and INPP4B. Data from case and control tissue biopsies were normalized on a commercial pool of control tissue biopsies from esophagus. Student's t-test was performed and P values are indicated. Bars indicate standard deviations.

164x209mm (300 x 300 DPI)

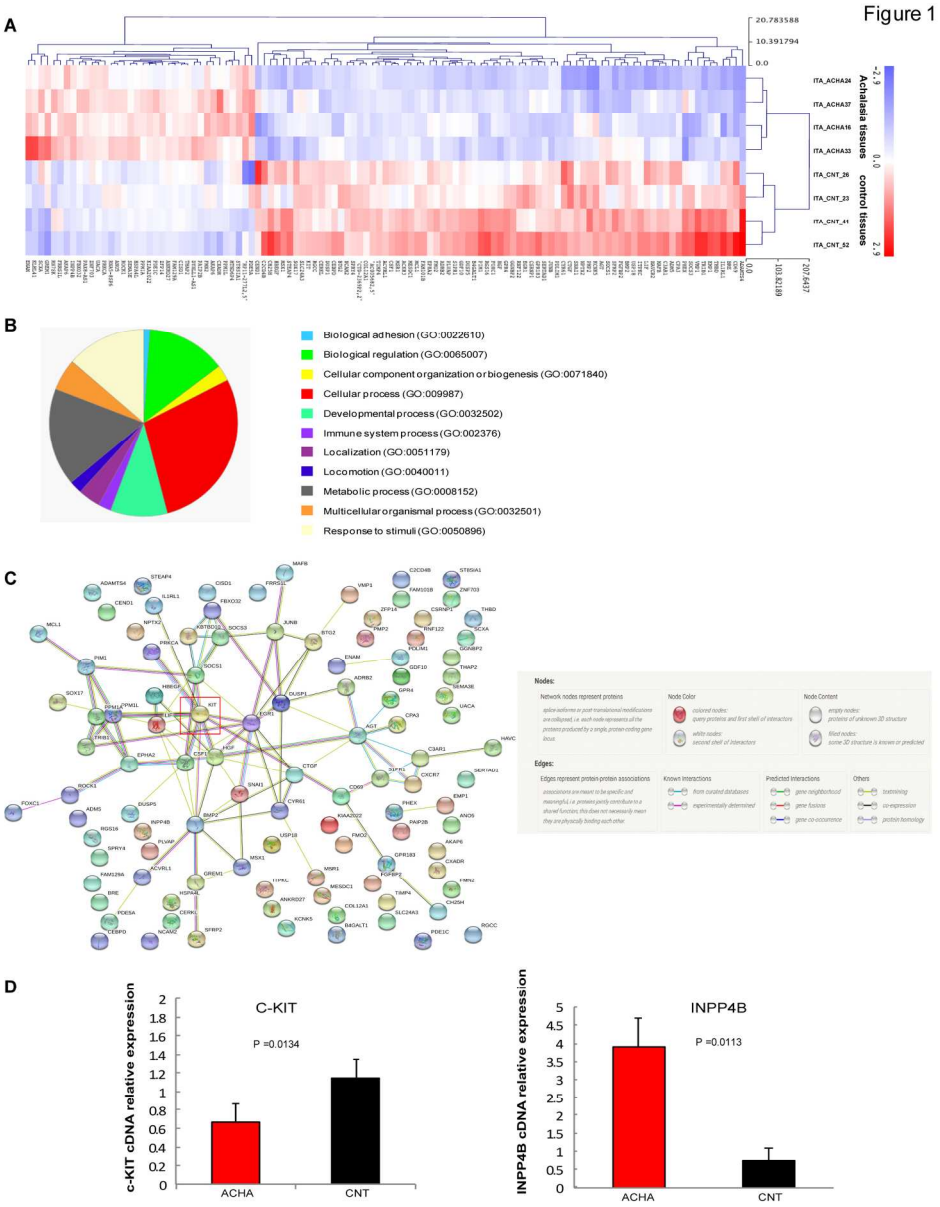

Figure 1. Differentially expressed genes in achalasia tissue. (A) Heat map showing the concordant differential expression observed in the tissues from achalasia patients compared to controls (for the genes reported in Table 1). Elaborated with MeV v4.8.1. (B) Biological processes of genes (GO-Slim Biological processes) differentially expressed in achalasia, as identified by PANTHER Functional Classification analysis. (C) Graphical output of significantly enriched protein-protein interactions determined with STRING analysis, showing the results of the 104 out of 111 dysregulated genes in achalasia, compared with data present in the STRING databases. The different colors in the figure inset identify the evidence for the different interactions (known; predicted; identified with other means, such as co-expression, data mining, and protein homology). The red square indicates c-KIT. (D) Real-time qRT-PCR data for c-KIT and INPP4B. Data from case and control tissue biopsies were normalized on a commercial pool of control tissue biopsies from esophagus. Student's t-test was performed and P values are indicated. Bars indicate standard deviations.

164x209mm (300 x 300 DPI)

Figure 2

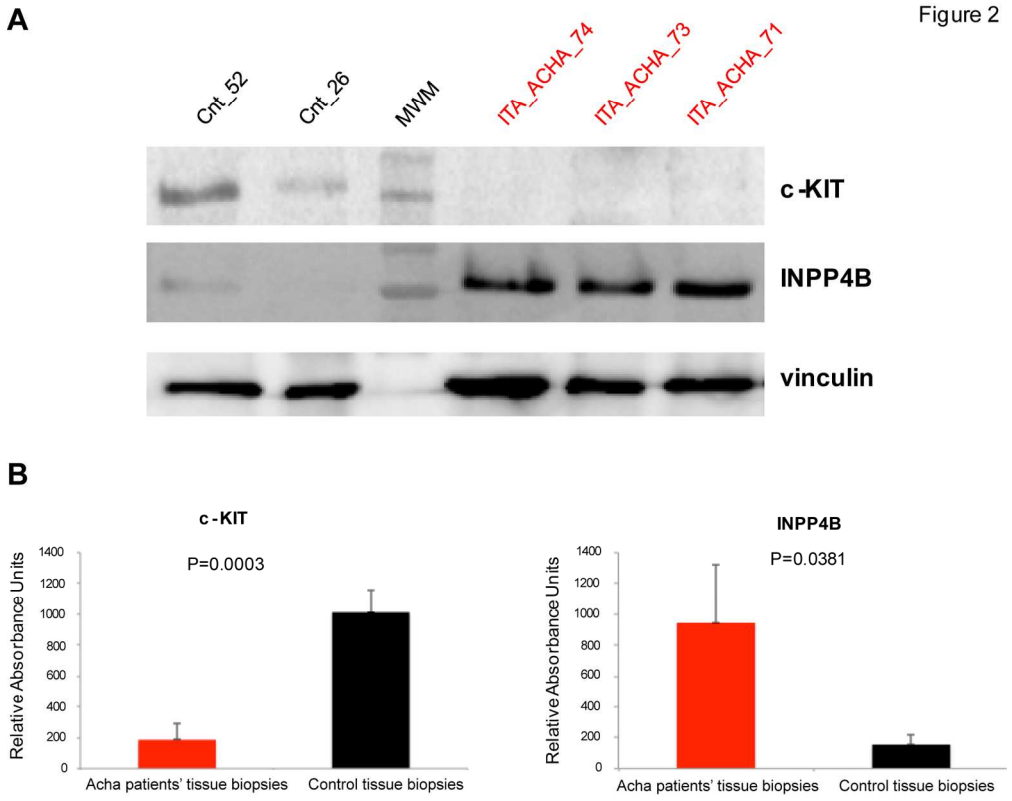

Figure 2. Western blot analysis of differentially expressed genes. (A) Example of the protein expression profiles in achalasia tissues compared to control samples for c-KIT and INPP4B. Western blotting was repeated in at least two independent experiments. (B) Densitometric analysis of the relative intensities for c-KIT and INPP4B. Quantitative data (mean values ± standard deviation) from different experiments obtained from each individual were compared using Student's t-test for statistical analysis. For each sample, densitometric values were normalized on reference protein (vinculin). All experiments were carried out at least twice. Bars indicated standard deviations. P values are indicated in the graphs.

160x126mm (300 x 300 DPI)

Figure 3

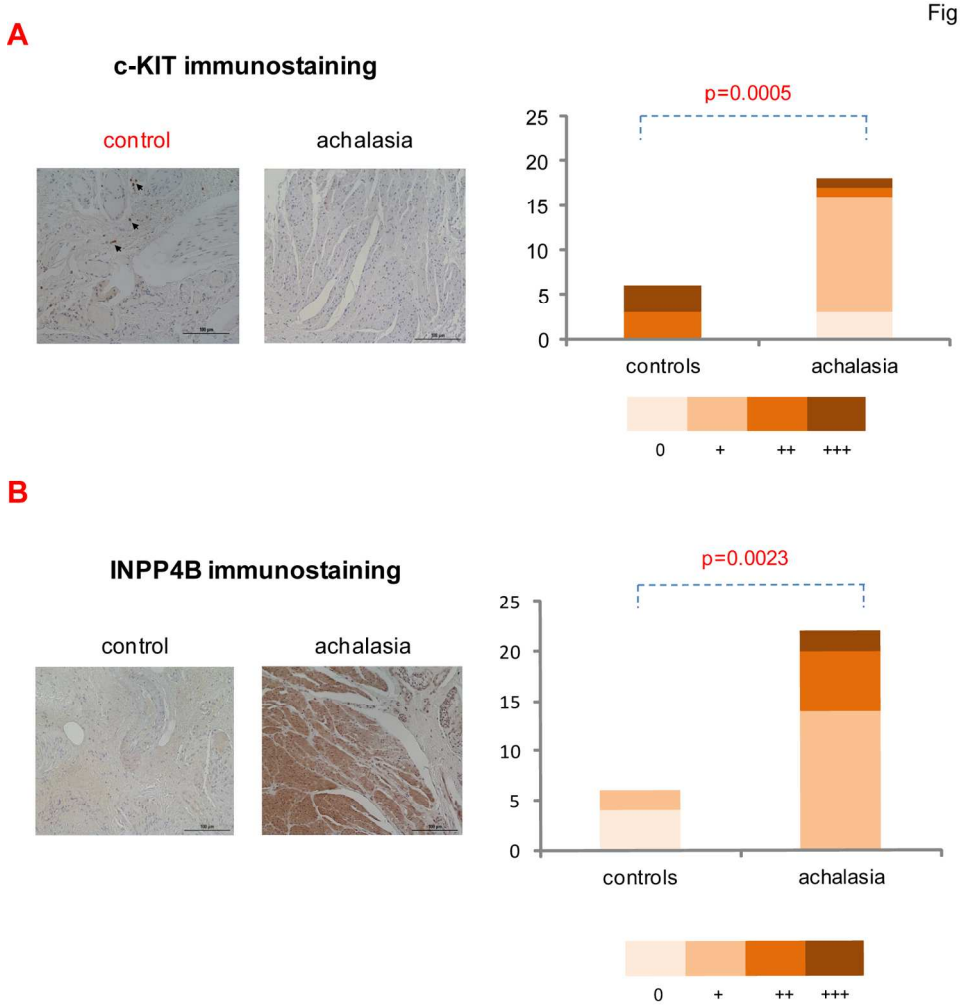

Figure 3. Immunostaining for c-KIT (A) and INPP4B (B). (A) Examples of the expression pattern for c-KIT in tissue biopsies from control (left) and achalasia patients (right). Arrows indicate the positive staining for c-KIT. c-KIT staining color histograms of controls (n=6) and cases (n=18) represent the number of samples assessed according to the semi-quantitative score. c-KIT immunolabeling differences in cases vs. controls were assessed by Fisher's exact test. (B) Examples of the expression pattern for INPP4B in tissue biopsies from control (left) and achalasia patients (right). INPP4B staining color histograms of controls (n=6) and cases (n=22) represent the number of samples assessed according to the semi-quantitative score. INPP4B immunolabeling differences in cases vs. controls were assessed by Fisher's exact test. Scale bars are 100μm as indicated.

159x160mm (300 x 300 DPI)

Figure 3

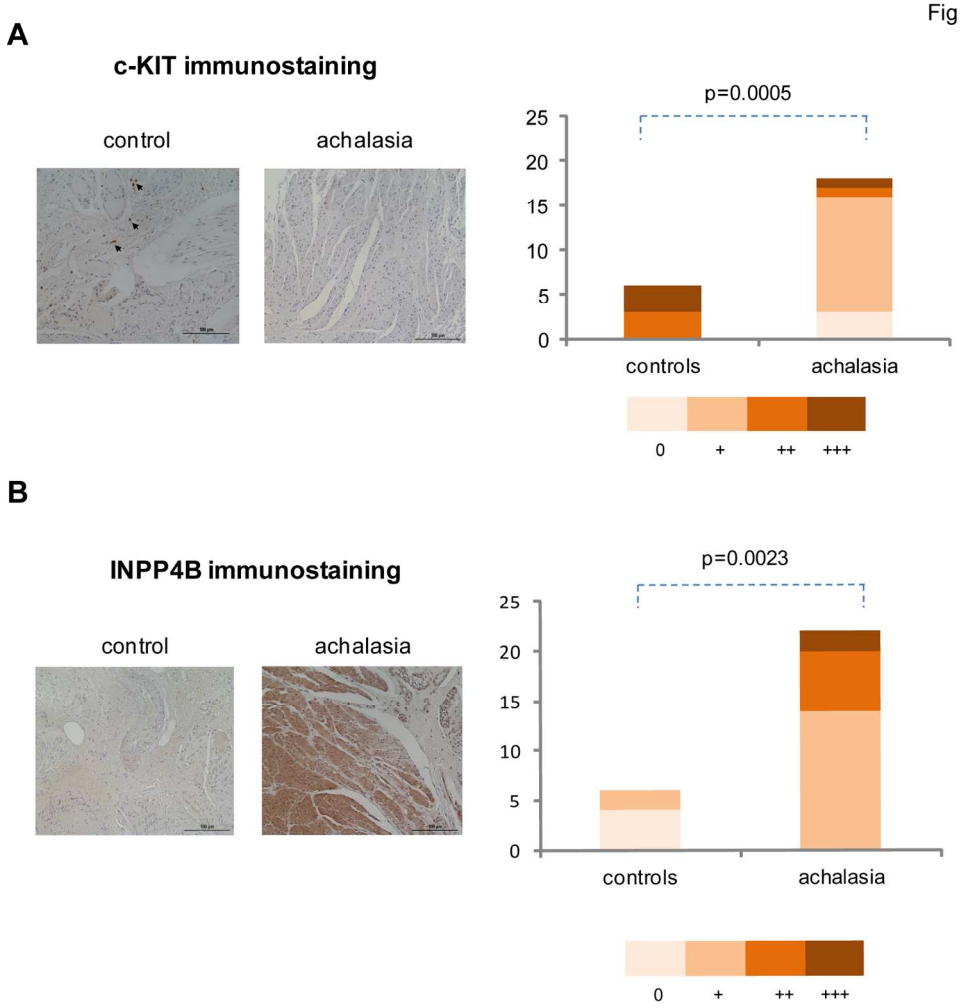

Figure 3. Immunostaining for c-KIT (A) and INPP4B (B). (A) Examples of the expression pattern for c-KIT in tissue biopsies from control (left) and achalasia patients (right). Arrows indicate the positive staining for c-KIT. c-KIT staining color histograms of controls (n=6) and cases (n=18) represent the number of samples assessed according to the semi-quantitative score. c-KIT immunolabeling differences in cases vs. controls were assessed by Fisher's exact test. (B) Examples of the expression pattern for INPP4B in tissue biopsies from control (left) and achalasia patients (right). INPP4B staining color histograms of controls (n=6) and cases (n=22) represent the number of samples assessed according to the semi-quantitative score. INPP4B immunolabeling differences in cases vs. controls were assessed by Fisher's exact test. Scale bars are 100μm as indicated.

159x160mm (300 x 300 DPI)

Figure 4

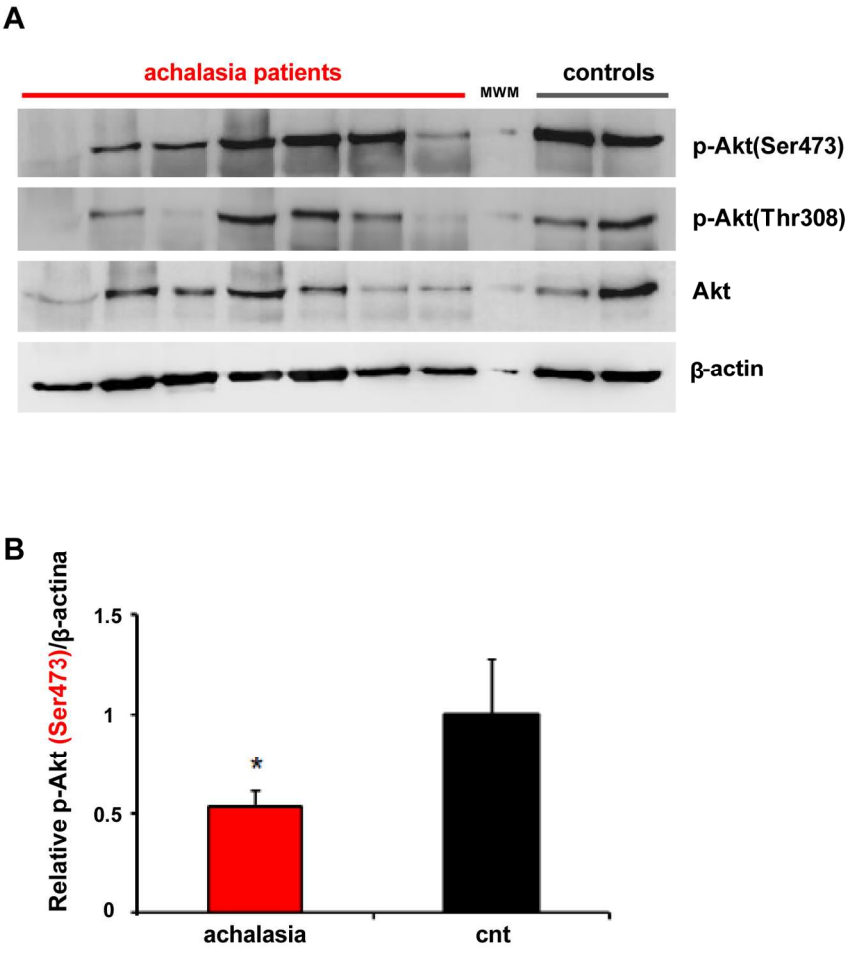

Figure 4. Phospho-Akt is down regulated in achalasia. (A) Example of the protein expression profiles in achalasia tissues compared to control samples of phospho-Akt (Ser473; Thr308) and total Akt. (B) Quantitative data (mean values ± standard deviation) from different experiments (performed in duplicate) obtained from each individual were compared using Student's t-test. For each sample, densitometric values were normalized on reference protein (β-actin). The significantly different relative phospho-Akt (Ser473) levels comparing achalasia vs. control tissues, were reported in the histogram (P=0.0495, Student's t-test). Bars indicate standard deviations.

159x154mm (300 x 300 DPI)

Figure 4

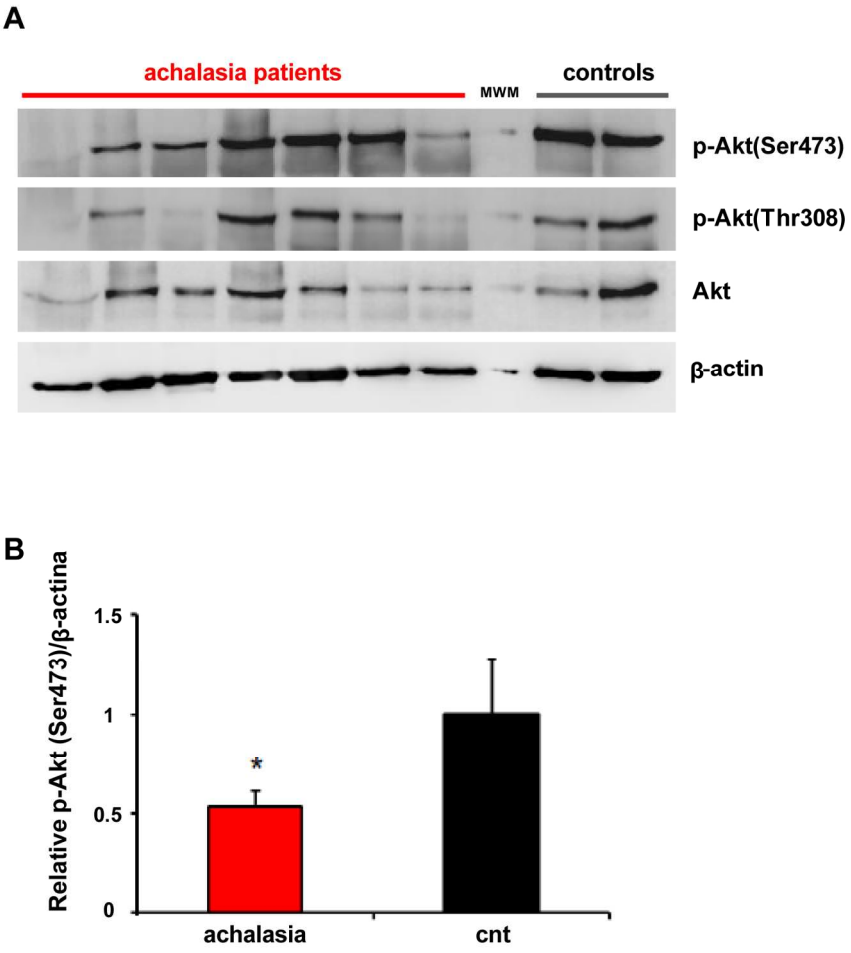

Figure 4. Phospho-Akt is down regulated in achalasia. (A) Example of the protein expression profiles in achalasia tissues compared to control samples of phospho-Akt (Ser473; Thr308) and total Akt. (B) Quantitative data (mean values ± standard deviation) from different experiments (performed in duplicate) obtained from each individual were compared using Student's t-test. For each sample, densitometric values were normalized on reference protein (β-actin). The significantly different relative phospho-Akt (Ser473) levels comparing achalasia vs. control tissues, were reported in the histogram (P=0.0495, Student's t-test). Bars indicate standard deviations.

159x154mm (300 x 300 DPI)